3106-1

GERMAN - MONGOLIAN INSTITUTE FOR RESOURCES AND TECHNOLOGY

The present work was submitted to
the German-Mongolian Institute of Resources and Technology

DESIGN AND ANALYSIS OF A HYBRID RENEWABLE MICROGRID SYSTEM FOR MINE SITES IN SOUTHWEST OF MONGOLIA

Masters Thesis

By

ERDENETSOGT Turbat

Study program: Master of Business Administration (MBA) in International Management of Resources and Environment

Student ID: 15367133731999

1st Supervisor/Examiner: Prof. Ariunbolor Purvee

2nd Supervisor/Examiner: Prof. Dr. Thomas Hollenberg

Ulaanbaatar/Nalaikh

2023

GERMAN - MONGOLIAN INSTITUTE FOR RESOURCES AND TECHNOLOGY

The present work was submitted to

the German-Mongolian Institute of Resources and Technology

DESIGN AND ANALYSIS OF A HYBRID RENEWABLE MICROGRID SYSTEM FOR MINE SITES IN SOUTHWEST OF MONGOLIA

Masters Thesis

By

ERDENETSOGT Turbat

Study program: Master of Business Administration (MBA) in International Management of Resources and Environment

Student ID: 15367133731999

1st Supervisor/Examiner: Prof. Ariunbolor Purvee

2nd Supervisor/Examiner: Prof. Dr. Thomas Hollenberg

Ulaanbaatar/Nalaikh

2023

Statutory Declaration

Erdenetsogt Turbat	15367133731999
First Name, Last Name	Student ID Number

I hereby affirm in lieu of an oath that I provided the submitted bachelor thesis

DESIGN AND ANALYSIS OF A HYBRID RENEWABLE MICROGRID SYSTEM FOR MINE SITES IN SOUTHWEST OF MONGOLIA

I did not use any sources other than those stated. In case that the work is additionally submitted on a data medium, I declare that the written and the electronic form are completely identical. The work was not submitted in the same or similar form to any examination authority.

June 4th, 2023	
Place, Date	Signature

Acknowledgment

First and foremost, I am grateful to my supervisors, Professor Ariunbolor Purvee and Professor Thomas Hollenberg, for their constant support, direction, and encouragement in completing this master's thesis. During difficult times, their enthusiasm and leadership provided me with the necessary mental and academic support.

Also, I would like to thank my wife and son for continually motivating me and assisting me in maintaining concentration during my master's thesis journey. Their encouragement was vital in keeping me focused and determined.

Finally, I want to express my heartfelt thanks to GMIT (German Mongolian Institute for Resources and Technology), where I had the opportunity to gather invaluable experience, broaden my academic knowledge, and hone my soft skills during my academic years. GMIT's learning environment and possibilities have extensively helped my personal and educational growth.

Abstract

This thesis focuses on the design and analysis of a renewable microgrid system for mines in the southwest of Mongolia, with an emphasis on addressing the energy-intensive nature of mining, diesel use, and CO2 emissions.

As a country abundant in renewable energy resources, Mongolia presents a unique opportunity to achieve sustainable solutions in the mining sector. However, despite proven renewable technology and a renewable-rich country, most mining companies have yet to adopt renewable solutions.

The methodology employed in this study encompasses several key steps. Firstly, an overview of the legal frameworks and regulations pertaining to renewable energy deployment in the mining sector in Mongolia is conducted. Next, a concept design phase is undertaken, integrating solar, wind, energy storage, and diesel generators to create an off-grid hybrid system tailored to the mine's energy requirements. Considerations such as load demand, resource availability, and system reliability are taken into account during the design phase. Modeling and simulation techniques are employed to assess performance and feasibility, evaluating various scenarios to meet energy needs while minimizing diesel fuel usage and CO2 emissions.

Furthermore, a detailed business case is developed, considering the initial capital investment, operational costs, and potential financial benefits of the renewable microgrid system. The analysis includes factors such as the payback period, return on investment (ROI), and levelized cost of electricity (LCOE), providing insights into the economic viability of the system for mining operations in Mongolia.

The analysis revealed that incorporating a wind turbine in the off-grid hybrid system increased the renewable energy fraction from 28.6% (PV + energy storage) to 88.1% (PV + energy storage + wind turbine), resulting in a significant reduction in the levelized cost of electricity (LCOE) and operating costs over the life of the mine.

However, PV energy systems with a peak capacity of 6 MW offered a more reliable and consistent energy source compared to wind turbines due to low wind speeds and higher installation costs associated with taller hub heights (>50m).

Table of Contents

1 Introduction and Motivation

The mining sector consumes a significant amount of energy globally, accounting for 11% of total global energy consumption and generating 4-7% of total greenhouse gas emissions annually (GHG) (Ellabban & Alassi, 2021). Typically located in rural areas, these mines often rely heavily on fossil fuels and must transport diesel over long distances to power on-site generators, which can significantly impact operating costs due to fluctuations in diesel prices (Ellabban & Alassi, 2021).

However, with increasing fossil fuel prices and advancements in renewable energy systems, there has been a shift towards integrating renewables at mine sites.

Globally, 1 GW of renewable energy systems (RES) have already been installed at existing mines, with another 1 GW in the pipeline (Paolo & Kevin, 2017).

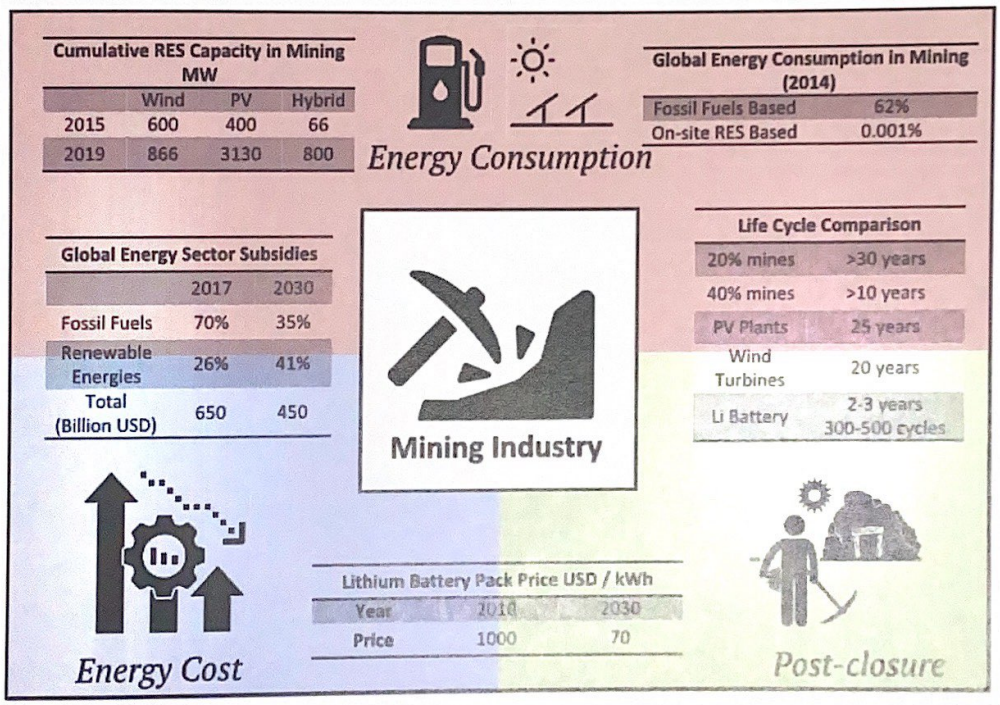

Figure 1: Comparative indicators pertaining to RES integration in mining (Gómez et al., 2020).

When solar Photovoltaic (PV) electricity is combined into a hybrid mining power plant, these types of systems can save up to 25-30%, and up to 70% in locations where diesel is more expensive (Pollack & Bongaerts, 2020).

Renewable hybrid microgrid systems, which offer reliability, cost-effectiveness, and environmental sustainability, are now being considered for mining projects in remote areas of Southwest of Mongolia (ROMA, 2020).

The motivation behind my thesis is to design and demonstrate a successful off-grid hybrid microgrid system for mining operations in Mongolia. By showcasing the feasibility and benefits of this solution, I aim to inspire mining companies to embrace sustainable practices and contribute to climate change mitigation. Given the energy-intensive nature of mining, utilizing renewable energy sources presents a viable and practical approach to reduce diesel consumption and unlock new opportunities for more sustainable mining practices. Through this thesis, I aspire to drive positive change in the mining industry by promoting the adoption of renewable energy solutions and fostering a more sustainable approach to mining in Mongolia.

1.1 State of Art

1.1.1 Hybridization in Mines Energy Production

Hybridization involves the integration of multiple energy sources, both renewable and non-renewable, to create a more reliable and cost-effective energy system. Solar panels, wind turbines, and energy storage devices, as well as traditional fossil fuel sources such as diesel and gas engines, can be used in mining applications as hybrid RES (Kim et al., 2011).

The choice of energy sources to integrate into the system depends on many factors. Those include the mine location, the energy demand, and the availability of renewable resources at the site.

Hybrid RES can provide significant benefits for mining operations such as reducing the cost of energy production, lower GHG, and increase the reliability of the energy supply. Nonetheless, developing and operating these systems may be challenging and often requires careful consideration of factors such as the energy demand profile, the sizing of energy storage (ESS) systems, and the control of power electronics.

1.1.2 Use of Homer Pro for Microgrid Systems and Mine Planning

HOMER Pro is a software tool that is widely used in the design and analysis of microgrids, particularly those that incorporate renewable energy sources (HOMER Pro, 2023b).

The software allows users to model the performance of different energy systems, and to optimize their design based on factors such as cost, energy demand, and the availability of renewable resources (HOMER Pro, 2023b).

In the mining sector, HOMER Pro is increasingly being used to plan and optimize microgrid systems that incorporate renewable energy sources, including solar and wind energy. By modeling the performance of different energy systems, mining companies can identify the most cost-effective and sustainable energy solutions for their operations (HOMER Pro, 2023b).

Authors use HOMER Pro to design and analyze the performance of a microgrid that integrates a solar PV system and a diesel generator set for a remote mining operation in China. As a result, the hybrid system provided reliable and cost-effective power to the mining operation, with a total cost of energy of $0.4/kWh. The system also reduced

greenhouse gas emissions by 1200 tons per year compared to a diesel-only system (HOMER Pro, 2023b).

1.2 Problem statement

This master's thesis aims to develop a concept design and analysis of a hybrid renewable microgrid system to meet energy demand at mine sites in southwest Mongolia in an energy-efficient, environmentally friendly way and thereby achieve a reduction in operating costs by reducing dependency on diesel fuel.

1.3 Objectives

The objectives of this thesis are as follows:

1. Review studies on hybrid renewable microgrid system performance, operation, and working conditions.
2. Review Mongolia's renewable energy laws, regulations, and standards.
3. Run HOMER Pro simulation and compare different off-grid microgrid case scenarios.
4. Analyze the optimal hybrid microgrid configuration, cost savings, payback period, and CO2 emissions reduction.
5. Conduct market research on key suppliers and develop business case respectively.

These objectives will contribute to find the most cost-effective, reliable, and advanced energy solution for mine sites in the southwest of Mongolia.

2 Microgrid

2.1 Overview

Renewable microgrid systems are small-scale energy systems that produce electricity from solar, wind, hydroelectric, or biomass renewable sources (Microgrid Institute, 2020). These systems typically include energy storage technologies and load management systems and are designed to operate with or without connection to the national grid (Microgrid Institute, 2020).

In a renewable microgrid system, energy is generated from the renewable sources and then stored in batteries or other energy storage devices (Zhou et al., 2015). The energy is then distributed to the local community or facility through a distribution network (Zhou et al., 2015). Load management systems are used to control the energy demand and ensure that the energy supply matches the energy demand (Zhou et al., 2015).

Nowadays, renewable microgrid systems have become crucial in the context of Mongolia's energy system because the country is highly dependent on fossil fuels in order to generate electricity, which causes many environmental and public health issues such air pollution (Saranchimeg et al., 2018).

According to a report by the United Nations Development Programme (UNDP), Mongolia has the potential to generate more than 400 gigawatts of solar power, which is equivalent to 280 times the country's current electricity consumption (UNDP, 2013).

Renewable microgrid systems have the potential to help Mongolia in reducing the country's reliance on fossil fuels, increasing energy security and independence, and contributing to the country's climate change initiatives (UNDP, 2013).

Renewable microgrids can also provide reliable and affordable energy to remote and off-grid communities which currently lack access to electricity (UNDP, 2013).

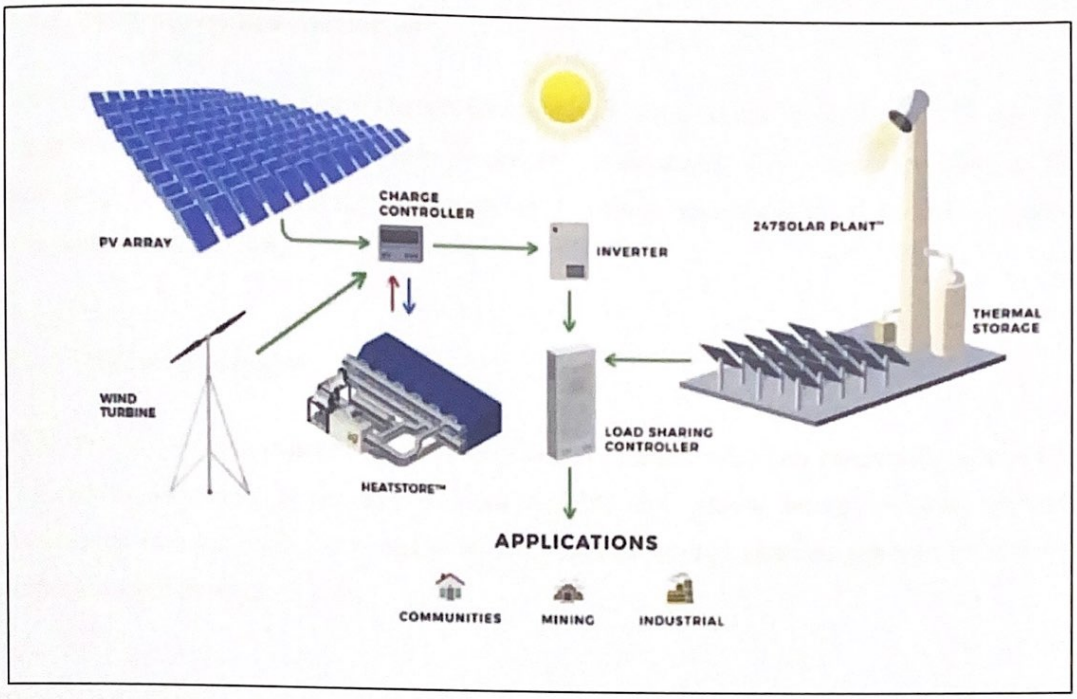

Figure 2: Layout for Hybrid Microgrid System for Mine Application (Media, 2021).

2.2 Application and Configurations

Renewable microgrid systems have a wide range of applications and can be configured in various ways to meet specific energy needs.

According to a report by the Institute of Electrical and Electronics Engineers (IEEE) and National Renewable Energy Laboratory (NREL), some common applications and configurations of renewable microgrids include.

2.2.1 Islanded microgrid

This configuration operates independently from the main grid and typically includes renewable energy sources, energy storage, and load management technologies (Rezkallah et al., 2019). Islanded microgrids can provide reliable and secure power to remote or off-grid communities and critical infrastructure such as hospitals and military bases (Rezkallah et al., 2019).

2.2.2 Grid-connected microgrid

This configuration is connected to the national grid, but it is able to operate on its own in the event of a grid outage or failure (Rezkallah et al., 2019). Grid-connected microgrids can help to increase energy resilience and reduce the impacts of power outages (Rezkallah et al., 2019).

2.2.3 Hybrid microgrid

This configuration combines multiple sources of energy, including renewable and non-renewable sources, to provide a more reliable and stable energy supply. Hybrid microgrids can be useful in areas where renewable energy sources are intermittent or unreliable (Zhou et al., 2015).

2.2.4 Campus or community microgrid

This configuration is designed to serve a specific campus or community and typically includes renewable energy sources, energy storage, and load management technologies (Zhou et al., 2015). Campus or community microgrids can help to reduce energy costs and increase energy independence.

In summary, renewable microgrid systems are becoming increasingly popular due to their potential to provide reliable, clean, and affordable energy. They offer several benefits over traditional grid systems, including increased energy efficiency, reduced GHG emissions, and improved energy reliability and security.

2.3 Advantages and Disadvantages

Renewable microgrid systems have several advantages and disadvantages, which should be considered when evaluating their potential as an energy solution (Hirsch et al., 2018).

Advantages:

1. Increased energy independence and security: Renewable microgrids can operate independently or in conjunction with the main grid, providing a more secure and reliable energy supply (Hirsch et al., 2018).
2. Reduced greenhouse gas emissions: Renewable microgrids use clean and renewable energy sources, which can help to reduce greenhouse gas emissions and mitigate climate change (Hirsch et al., 2018).
3. Lower energy costs: Renewable energy sources are becoming increasingly cost-competitive with traditional energy sources, which can help to reduce energy costs over the long-term (Hirsch et al., 2018).
4. Improved energy efficiency: Renewable microgrids can use energy storage and load management technologies to optimize energy use and reduce waste (Hirsch et al., 2018).

Disadvantages:

1. High upfront costs: The initial investment required to install a renewable microgrid can be higher than that of traditional energy systems (Hirsch et al., 2018).
2. Intermittency of renewable energy sources: Renewable energy sources such as solar and wind are intermittent and can be affected by weather patterns, which can lead to variability in energy supply (Hirsch et al., 2018).
3. Maintenance and operational challenges: Renewable microgrids require regular maintenance and monitoring to ensure optimal performance, which can be challenging in remote or off-grid locations (Hirsch et al., 2018).
4. Limited scalability: Renewable microgrids are typically designed for small-scale applications and may not be suitable for large-scale energy needs (Hirsch et al., 2018).

3 Components of Microgrid

Microgrids are small-scale power systems that can operate independently or in connection with the main grid. They typically consist of multiple distributed energy resources (DERs) and loads, as well as energy storage and control systems.

The below table demonstrates the overview of the components that make up a microgrid.

Table 1: Microgrid Components (Microgrid Institute, 2020).

Distributed Energy Resources (DERs)	DERs are small-scale power generation units that are located close to the load they serve. They can include solar panels, wind turbines, microturbines, fuel cells, and small-scale hydroelectric generators.
Energy Storage Systems	Energy storage systems are used to store excess energy generated by DERs for later use when demand exceeds supply. They can include batteries, flywheels, and pumped hydroelectric storage.
Loads	Loads are the devices or appliances that consume electricity. They can include lighting, heating and cooling systems, and industrial machinery.
Power Electronics	Power electronics are used to convert the DC power generated by DERs and stored in energy storage systems into AC power that can be used by loads. They can include inverters, rectifiers, and DC-DC converters.
Control Systems	Control systems are used to manage the operation of the microgrid, ensuring that supply and demand are balanced and that the system operates efficiently and reliably. They can include supervisory control and data acquisition (SCADA) systems, energy management systems (EMS), and distributed control systems (DCS).

4 Overview of Mongolian Energy System

Mongolia is a landlocked country located in Central Asia with a population of approximately 3.348 million people as of today. The country has abundant natural resources, including coal, oil, natural gas, and renewable energy sources such as wind, solar, and hydropower.

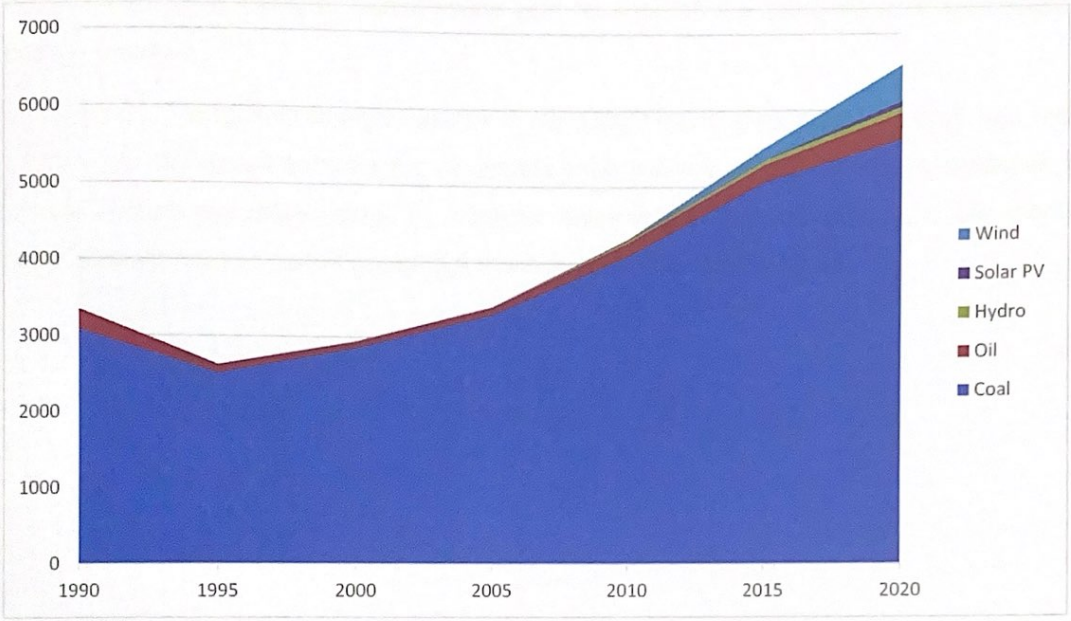

Figure 3: Electricity generation by source, Mongolia 1990-2020 (IEA, 2023).

Historically, Mongolia's energy system has been heavily dependent on coal, which accounts for over 90% of the country's electricity generation as shown in Figure 3.

The majority of Mongolia's coal reserves are located in the South Gobi region, where several large-scale coal mines have been developed in recent years to supply raw coal to China.

In addition to coal, Mongolia also has significant potential for renewable energy development. The country has abundant wind and solar resources, particularly in the Gobi Desert region, which is one of the world's best locations for wind and solar energy. Mongolia also has several solar, wind, and hydropower projects that feed into the main grid and generate electricity for local communities.

Despite its potential for renewable energy development, Mongolia faces several challenges in transitioning to a more sustainable energy system. These include limited transmission infrastructure to connect remote renewable energy projects to the grid,

inadequate regulatory frameworks to support renewable energy development, and limited access to financing for renewable energy projects.

To address these challenges, the Mongolian government has implemented several policies to promote renewable energy development, including feed-in tariffs, tax incentives, and renewable energy quotas. The government has also prioritized the development of a national transmission grid to support the integration of renewable energy projects.

In summary, Mongolia's energy system is currently heavily dependent on coal, but the country has significant potential for renewable energy development. The government and private sectors are taking steps to promote renewable energy development, but faces several challenges in transitioning to a more sustainable energy system.

5 A case study for the Agnew Hybrid Gold Mine in Australia

5.1 Introduction

The Agnew Hybrid Gold Mine is located in the Eastern Goldfields region of Western Australia and is owned and operated by Gold Fields Limited, a South African-based gold mining company (James, 2022). The mine has been in operation since 2005 and produces approximately 250,000 ounces of gold per year (James, 2022).

5.2 Energy System Overview

The Agnew Hybrid Gold Mine's energy system is a combination of grid-connected and off-grid power generation(James, 2022). The mine is connected to the Western Australian electricity grid, but also has a 23 MW gas-fired power plant on site to provide backup power in case of grid outages. In addition, the mine has recently installed a 4 MW solar power plant and a 13 MW battery storage system, making it one of the largest hybrid renewable energy systems in the world (James, 2022).

5.3 Hybridization of Energy Production

The hybridization of energy production at the Agnew Gold Mine has resulted in significant cost savings and environmental benefits (James, 2022). The mine's solar power plant and battery storage system are expected to reduce the mine's diesel consumption by approximately 10%, resulting in an estimated annual saving of $2-3 million. In addition, the use of renewable energy sources has reduced the mine's greenhouse gas emissions by approximately 40,000 tonnes per year (James, 2022).

5.4 HOMER Pro Used in Planning

HOMER Pro, a microgrid design and optimization software, was used in the planning and design of the Agnew Hybrid Gold Mine's renewable energy system (James, 2022). The software was used to analyze the mine's energy demand profile, identify the optimal sizing of the solar and battery systems, and optimize the dispatch of energy from the different sources (James, 2022).

5.5 Results and Discussion

The Agnew Hybrid Gold Mine's renewable energy system has been operational since 2019, and the results have been positive. The use of renewable energy sources has reduced the mine's reliance on diesel generators, resulting in lower fuel costs and reduced emissions. The solar power plant and battery storage system have also provided

a reliable source of power, reducing the risk of power outages and downtime at the mine. The use of HOMER Pro in the planning and design of the system has been critical in optimizing the system's performance and ensuring that it meets the mine's energy needs (James, 2022).

5.6 Conclusion

The Agnew Hybrid Gold Mine's renewable energy system is a successful example of the hybridization of energy production in the mining industry. As a result of using renewable energy sources, there were significant cost savings and environmental benefits, while also providing a reliable and secure source of power for the mine's operations. The use of HOMER Pro in the planning and design of the system demonstrates the importance of advanced modeling and optimization tools in the development of effective renewable energy systems.

6 Overview of Renewable Energy Law and Legal Frameworks for Hybrid Microgrids in Mongolia

Mongolia has made significant efforts towards promoting renewable energy development, with the government implementing various laws, regulations, and standards to support this sector.

The Law on Energy Conservation and Renewable Energy was first enacted in 2007, with the aim of promoting renewable energy development and reducing energy consumption. The law mandated the establishment of a Renewable Energy Fund to provide financial support for renewable energy projects, as well as the development of a Renewable Energy Standard to ensure the quality and safety of renewable energy systems (NREC, 2023).

In 2015, Mongolia adopted a National Renewable Energy Program with a goal of increasing the share of renewable energy in the country's energy mix to 20% by 2020 and 30% by 2030. The program outlines various policy measures, including feed-in tariffs, tax incentives, and simplified procedures for renewable energy project development (World Bank, 2017).

In addition to these overarching laws and policies, Mongolia has also established technical standards for renewable energy systems, including the Mongolian Wind Energy Standard and the Mongolian Solar Energy Standard. These standards specify technical requirements and safety measures for wind and solar energy systems, respectively (NREC, 2023).

As for hybrid renewable microgrid systems, there are currently no specific laws or regulations in place in Mongolia. However, the government has been exploring the potential of such systems in the country's remote areas, where the grid is unreliable or absent. The National Renewable Energy Center of Mongolia has been conducting pilot projects to test the feasibility of hybrid renewable microgrid systems in these areas, with the aim of providing clean and reliable energy access to local communities (NREC, 2023).

In terms of best practices, there are several international organizations and initiatives that provide guidelines and standards for renewable energy and microgrid systems.

For example, the International Electrotechnical Commission (IEC) has published standards for microgrid systems, including IEC 61850, which specifies communication protocols for microgrid control systems (Microgrid Institute, 2020). The Microgrid Institute also provides a framework for microgrid development, including technical, economic, and regulatory considerations (Microgrid Institute, 2020).

Mongolia has made significant progress in promoting renewable energy development; however, there is still room for improvement in terms of specific laws and regulations for hybrid renewable microgrid systems.

Looking to international best practices and standards for guidance in developing a legal framework for such systems in Mongolia may be beneficial.

7 Concept Design and Site Analysis for Bayankhundii Microgrid System

As mentioned earlier, the mining operations in Southwest Mongolia are typically located in remote areas with an unstable or absent national grid.

Consequently, diesel generators are commonly employed to power facilities in these regions. However, relying on diesel generators for energy production is both expensive and environmentally unsustainable.

In this section, we will delve into the feasibility of implementing a microgrid hybrid renewable system at one of these mining sites.

Our analysis will involve assessing the viability of utilizing available natural resources, such as wind and solar energy.

Additionally, we will consider factors such as the site's specific load profile to determine the optimal renewable energy mix.

7.1 Site Survey

7.1.1 Site location

The Bayankhundii Project is located in the southwestern region of Mongolia, approximately 980 km from the country's capital, Ulaanbaatar and about 300 km south of Bayankhongor Province, as illustrated below in Figure 4.

This project is based within the Khundii Gold District, an emerging gold region that encompasses the Bayan Khundii gold deposit, the Altan Nar gold-polymetallic deposit, the Zuun Mod copper-molybdenum deposit, and a range of mineral occurrences currently undergoing exploration by Erdene (ROMA, 2020).

Due to the remote location of this project site, the national grid infrastructure is either unstable or non-existent (ROMA, 2020).

Consequently, power generation is primarily dependent on diesel generators, which are one of the most expensive and environmentally unsustainable way to generate electricity.

We will assess the feasibility of installing a microgrid hybrid renewable energy system that utilizes available natural resources, such as solar, and wind energy and diesel, while considering the site's load profile in the following sections.

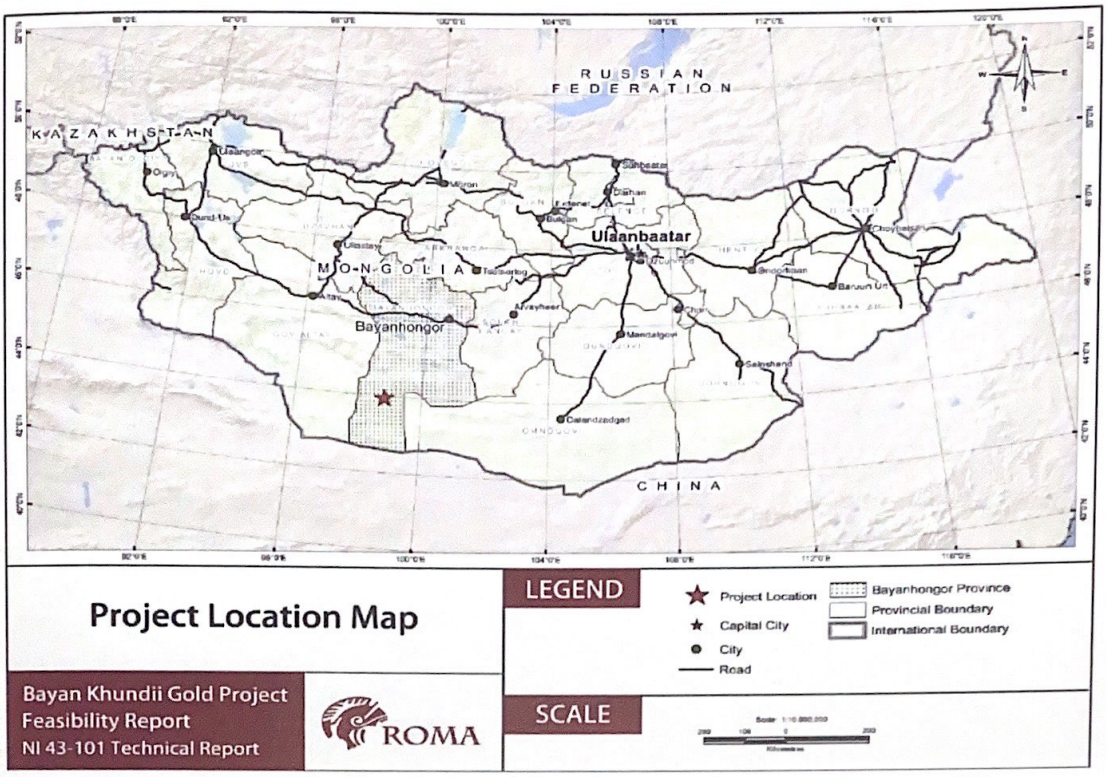

Figure 4: Location of the Project (ROMA, 2020).

7.1.2 Mine site review

According to their feasibility study, the mine site will consist of several large buildings and constructions including 30 x 18-meter office, bus shelter, security guard house, mine dry, 24 x 24-meter warehouse, chemical storage, workshop, and so on.

The accommodation camp will be located roughly 6 kilometers north of the Process Plant, near the site access road. The accommodation camp will be created for rostered personnel and will have a capacity of 372 people (ROMA, 2020).

Figure 5: Drawings of Mine Workshop and Accommodation Village Render (ROMA, 2020).

7.2 Load data

According to Bayankhundii's feasibility study the proposed solution for meeting reliability and expected power needs on-site involves the use of a combined solar and diesel power generation system (ROMA, 2020).

The average load demand is estimated to be around 4+ MW, and the distribution of power on the premises will be transmitted at 6.6 kV through substations located in areas with significant power requirements (ROMA, 2020).

The selected power station, utilizing solar, diesel, and battery technologies, has been designed to provide a total installed load capacity of 6.29 MW. The maximum contracted electricity demand is set at 7.2 MW, while the estimated average demand is 6 MW. The primary substation will have a single 11 kV transformer that will feed power to the 11 kV distribution network (ROMA, 2020).

7.3 Load profile

The average load demand is 4 MW. However, we can anticipate a minor rise in power consumption during roster shift hours, which typically occurs twice a day. Unfortunately, we don't have specific data regarding the change in load during these hours, so we have assumed that the load remains constant for our calculations.

7.4 Monthly fluctuation of load and temperature profile

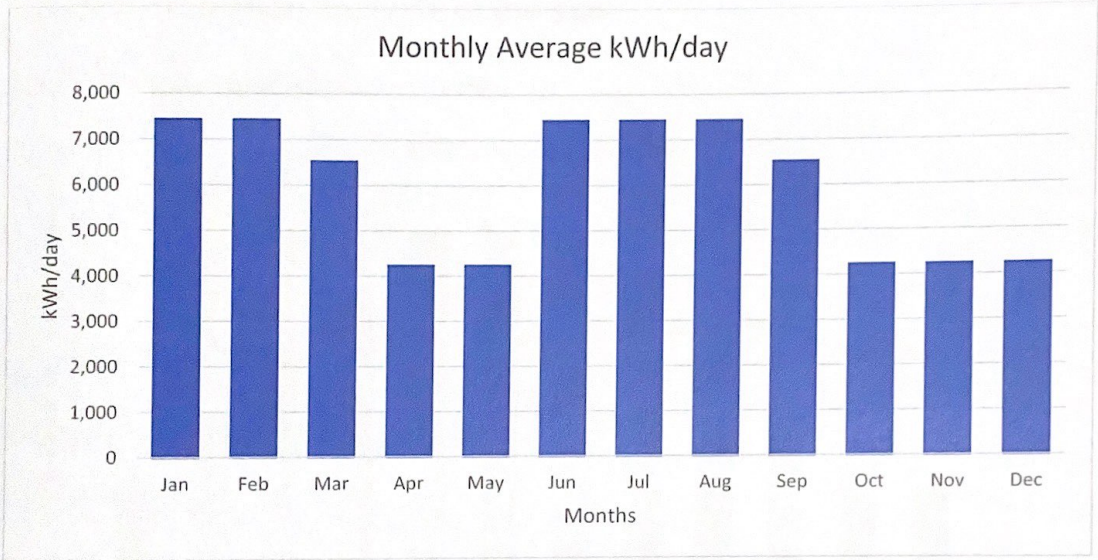

Figure 6: Monthly Average Daily Load Consumption

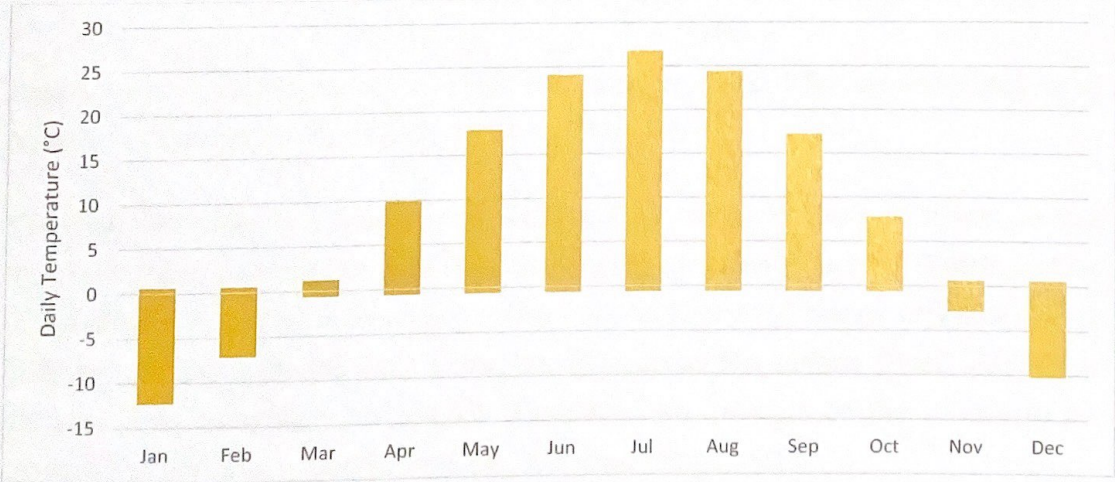

Figure 7: Monthly Average Temperature

Figure 6 and Figure 7 above shows the monthly fluctuation of load and temperature profile. When compared to other seasons, we can see that load demands are greater during the summer and winter seasons due to cooling and heating loads, respectively. This is because of a fully automated Central Heating Plant (CHP). The CHP will utilize 1 x coal fired 2.5 MW boiler for use in the winter at full load and 1 x 1.0 MW boiler for hot water in the summer months and back-up during the winter (ROMA, 2020).

7.5 Solar radiation analysis of the site

7.5.1 Monthly Solar Radiation Profile

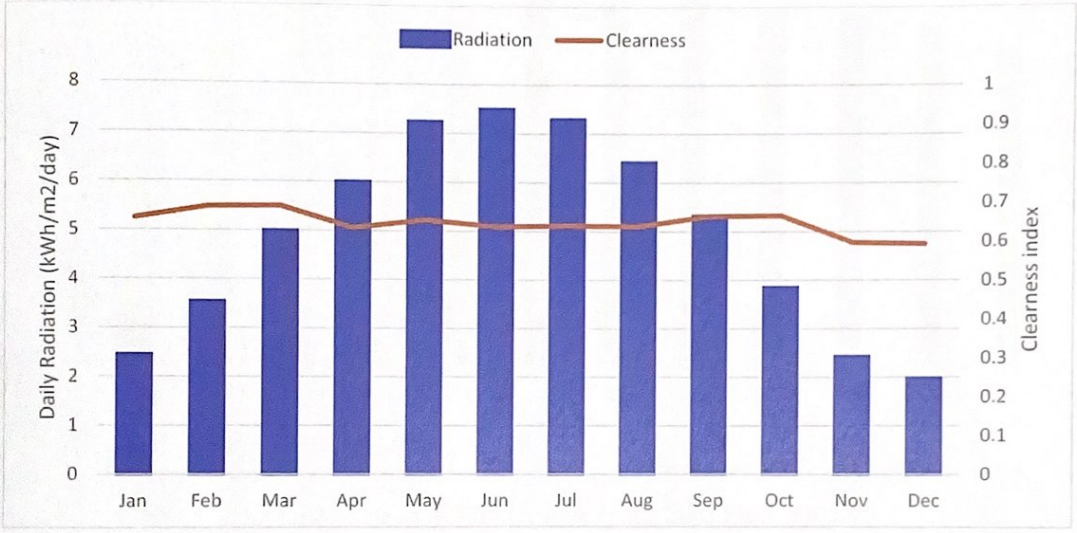

Figure 8: Daily Solar Radiation (Global Horizontal)

Figure 8 above displays monthly global horizontal irradiance. The average daily solar radiation calculated for Bayankhundii is 4.81 kWh/m2/day.

The clearness index is a way to measure how clear the atmosphere is. It tells us how much of the Sun's energy can pass through the atmosphere and reach the Earth's surface (Page, 2018). The index is a number between 0 and 1, where 0 means very little energy gets through and 1 means most of the energy reaches the surface (Page, 2018). We calculate it by comparing the amount of radiation we measure on the surface to the amount that would be expected from the Sun alone (Page, 2018).

7.6 Wind Analysis for Site

The amount of wind energy that can be harvested changes with the cube of the wind speed. As a result, understanding the characteristics of wind resources is critical for wind energy development in terms of identifying suitable sites and predicting economic viability. NASA's surface meteorological and solar energy databases were used to derive the wind data. The wind speed data for the terrain is for 50m above the earth's surface, averaged monthly over a ten-year period.

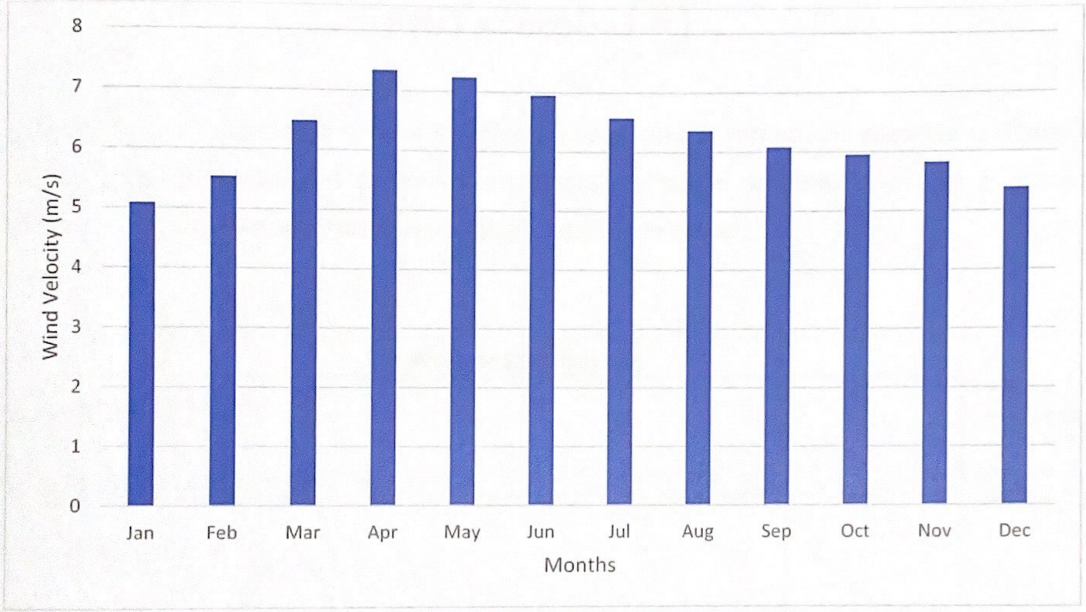

Figure 9: Average Wind Velocity @ 50m Hub Height

Figure 9 above displays the monthly fluctuation of wind speed. The average wind velocity is approximately 6.23 m/s for Bayankhundii mine site at 50m hub height.

7.6.1 Weibull Distribution Curve

Wind variability is one of its properties, both geographically and temporally (Denim, 2017). Many common sites use the Weibull distribution to characterize the fluctuation in hourly mean wind speed over a year (Denim, 2017).

The distribution can be mathematically represented as

$$F(U) = \exp\left(-\left(\frac{U}{c}\right)^{k}\right) \tag{1}$$

Where F(U) is the fraction of time for which hourly mean wind speed exceeds U (Denim, 2017). It is characterized by two parameters: a 'scale parameter' c and a 'shape parameter' k which describes the variability about the mean.

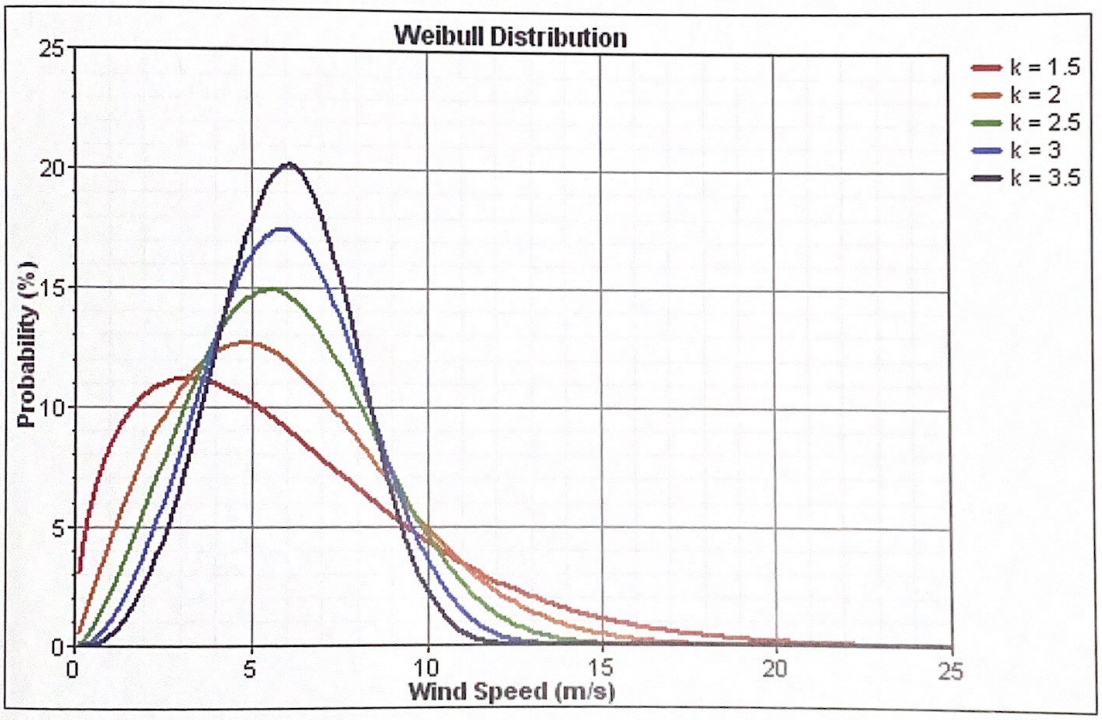

Figure 10: Weibull Distribution Curve at Average Wind Speed of 6 m/s

Figure 10 above displays the Weibull distribution for an average wind speed of 6m/s with different Weibull k value (Denim, 2017). The wind speed distribution is determined by the scale 'c' and form factor 'k'. As seen in the graph, higher k values correspond to a narrow

distribution of wind speed, whereas lower k values correspond to a broader distribution of wind speed. As a result, a place with consistent wind speed will have a higher k value (3 or 4), whereas a location with gusty wind will have a lower k value (1.5 or 1.2).

These variations are further influenced by changes in isolation throughout the year caused by the tilt of the earth's axis of rotation (Denim, 2017).

For our analysis, we use a k value of 2, which is common in many regions.

8 Modeling and Simulation Study for Bayankhundii Microgrid System

In this chapter, we will conduct modeling and simulation studies for several off-grid scenarios using HOMER Pro and HelioScope software.

In the off-grid system study, we will run simulations to determine the ideal configuration of the renewable hybrid system in order to save money and reduce diesel generator fuel consumption and CO2 emissions.

8.1 Homer Pro Simulation Software

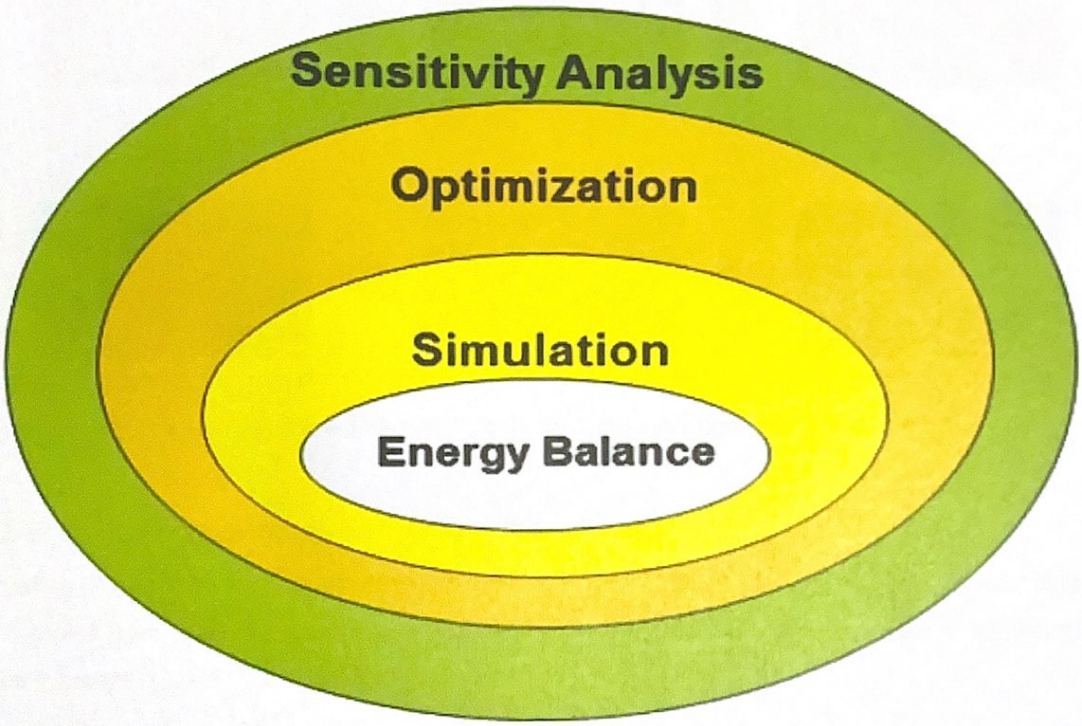

Figure 11: Homer Pro Simulation - Optimization- Sensitivity Analysis Tool (HOMER Pro, 2023b).

HOMER Energy's HOMER Pro® microgrid software is the trusted global standard for optimizing microgrid design across all industries (HOMER Pro, 2023b). The National Renewable Energy Laboratory (NREL) of the Department of Energy created the HOMER Pro Software in 1992, and it was privatized in 2009 (HOMER Pro, 2023).

The HOMER simulation performs an energy balance for each timestep of the year to determine how a specific system is expected to operate over the course of the project, as well as economic optimization by determining the least cost option based on the lowest net present cost (HOMER Pro, 2023).

8.2 Steps in Simulation of Microgrid

The following flow diagram demonstrates the arranged steps that I followed to conduct the simulation study of off-grid microgrid system for Bayankhundii Gold Project.

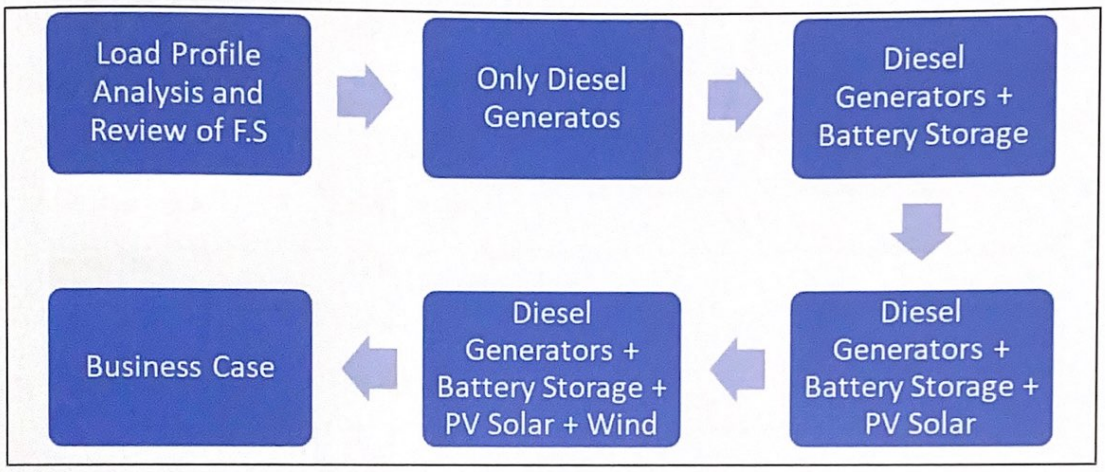

Figure 12: Flow Diagram Showing Steps in Microgrid Simulation

8.3 Input Parameters for Analysis

Below Table 1 shows the parameters that have been utilized for my analysis. According to latest data from the Central Bank of Mongolia, the country's discount rate is 13% and its inflation rate is 11%. (Mongolbank, 2023).

Table 2: Input Parameters for Simulation Study

Component	Capital/Replacement Cost	O & M Cost per Kw
PV	USD 2500/kW	USD 10/year
Converter	USD 300/kW	0
New Generators	USD 500/kW	USD 0.030/op.hr
Lithium-Ion Battery	USD 700/kW	USD 10/year
Wind	USD 2333/kW	USD 20/year
Other miscellaneous	USD 5000	
Other Parameters		
Project lifetime	15 years	
Diesel Fuel Price	USD 1/Liter	
Discount Rate	13%	
Inflation Rate	11%	
Generator Life Cycle	15,000 hrs.	

The input parameters, as indicated in

Table 2, have been finalized with up-to-date market information.

Several other cost metrics, such as capital and O&M (operation and maintenance), were also examined based on the literature review and HelioScope financial results.

All of the calculations were done with a 15-year project in perspective according to Erdene's feasibility report (ROMA, 2020).

The table below displays the different icons used to explain the results of the analysis in the following calculations.

Table 3: Description of Simulation Study Icons

Icons	Description
	Renewable fraction
	LCOE
	Initial Capital
	O & M Cost
	Fuel Cost
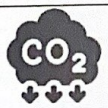	CO2 Emissions
	Discounted Payback Period

8.4 Off-Grid System Analysis

As shown in the flow diagrams on Figure 12 and Figure 13: Bayankhundii Off-Grid Microgrid Design Schematic (HOMER Pro, 2023b)., we will analyze the system consideration of being completely off-grid, i.e., having no access to the national grid in the following subsections.

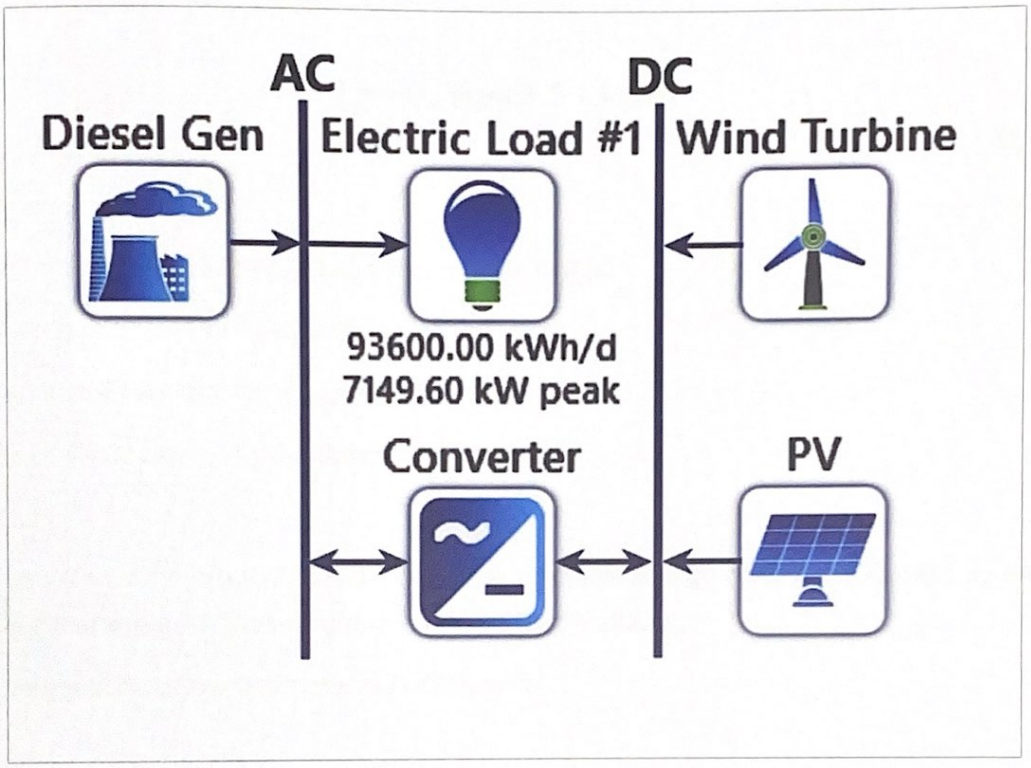

Figure 13: Bayankhundii Off-Grid Microgrid Design Schematic (HOMER Pro, 2023b).

Figure 13 above shows the final layout of the off-grid system. In the following sections, we will assess the system step by step, starting with a system that solely uses diesel generators and then adding storage, PV, and wind to compare the system output profile and savings achieved in each scenario.

8.4.1 Large DG (Diesel Generator)

The fuel curve describes how much fuel the generator uses to produce power. In the model, the linear function is used. For more than two points, a linear regression technique is employed to construct the line of best fit (Denim, 2017). The following equation calculates the generator's fuel consumption in units per hour as a function of its electrical output (HOMER Pro, 2023a).

$$F = F0.\ Ygen + F1.Pgen \tag{2}$$

Where,

F0 = the fuel curve intercept coefficient [units/hr/kW]

F1 = the fuel curve slope [units/hr/kW]

Y_{gen} = rated capacity of the generator [kW]

P_{gen} = the electrical output of the generator [kW]

The generator's electrical efficiency as the electrical energy coming out divided by the chemical energy of the fuel going in (HOMER Pro, 2023a).

The equation below describes the relationship

$$\eta_{gen} = \frac{3.6\ .\ P_{gen}}{\dot{m}_{fuel}\ .\ LHV_{fuel}} \tag{3}$$

Where,

P_{gen} = the electrical output [kW]

$\dot{m}_{fuel}$ = the mass flow rate of the fuel [kg/hr.]

LHV_{fuel} = the lower heating value (a measure of energy content) of the fuel [MJ/kg]

The factor of 3.6 arises because 1 kWh = 3.6 MJ.

After we ran the simulation to find the optimal generator size, it was found that in order to match the hourly load profile and, most importantly, the mine site peak load, we would require a minimum diesel generator capacity of 7900 kW (7.9 MW).

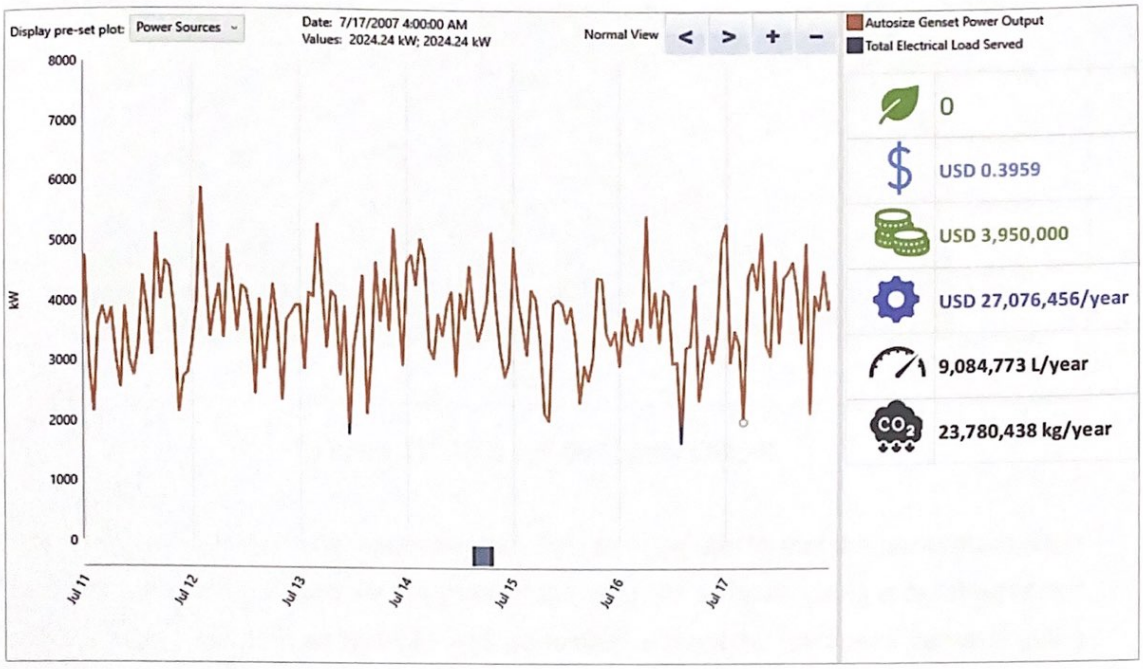

Figure 14: System Output Profile with DG

From Figure 14, we can observe that there is no excess electricity generated by DG as DG output is orange and load demand is blue colored line in the graph.

In fact, the result shows yearly excess electricity of 0.0962%, which in turn leads to no extra fuel consumption or operating cost.

According to Caterpillar, If DG is oversized, operating a diesel generator at load levels less than 25% of rated output for extended time periods impacts the unit negatively (CAT, 2023).

The most common result is engine exhaust slobber, also known as exhaust manifold slobber or wet stacking. Engine slobber is a black, oily liquid that can leak from exhaust manifold joints after extended periods of low or no load (CAT, 2023). These conditions can cause power losses, poor performance, and accelerated component wear, resulting in higher maintenance costs and unplanned downtime or failure (CAT, 2023).

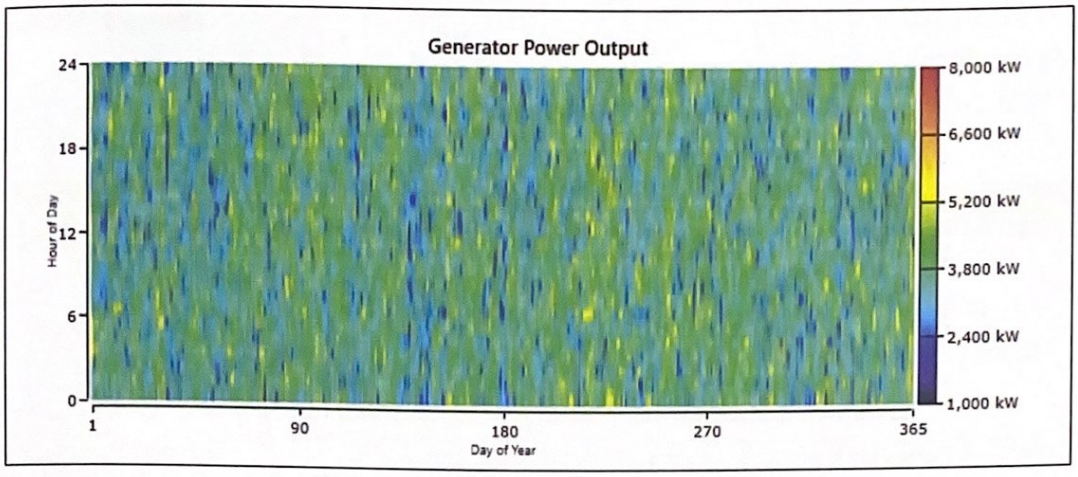

Figure 15: 7900 kW Generator Output

We can observe from the generator output data from Figure 15 that the generator power output is less than 3904kW for the most of the year. As a result, using a derating factor of 0.8 for the generator, an analysis was performed to meet the load/peak demand using a 7900-kW output capable generator.

8.4.2 Large DG + Energy Storage

The Idealized Storage Model is a replication of a straightforward storage model. It assumes a discharge curve that remains flat due to the predominantly constant supply voltage throughout the discharge cycle (HOMER Pro, 2023b). The model requires only the nominal capacity in amp-hours as input, which HOMER considers as the actual storage capacity. Notably, the Idealized Storage Model demonstrates good compatibility with certain high-performance Lithium-Ion batteries (HOMER Pro, 2023b).

To introduce a new storage component utilizing the Idealized Storage Model, the recommended approach involves duplicating an existing component that already incorporates this model, such as the Generic 1kWh Li-Ion battery. By modifying the variables specific to the new component, it can be tailored to meet the unique requirements and characteristics of the intended storage system. This methodology ensures an efficient process for creating and adapting storage components within the framework of the Idealized Storage Model (HOMER Pro, 2023b).

8.4.2.1 General

Table 4: Battery key terms explanations (HOMER Pro, 2023b).

Variable	Description
Nominal Voltage	The rated voltage. It is called nominal because the actual voltage varies according to the storage unit's operating conditions and state of charge. This input is used to convert specifications in A or Ah to values in kW or kWh.
Nominal Capacity	The rated capacity in amp hours. It is the total capacity of the storage system.
Round Trip Efficiency	The round-trip, DC-to-storage-to-DC efficiency of the storage bank. HOMER assumes that the percentage loss on charge and on discharge are the same.
Minimum State of Charge	The relative state of charge below which the storage bank is never drawn.
Maximum Charge Rate	The maximum allowable charge rate of the storage component, measured in amps per amp-hour of unfilled capacity.
Maximum Charge Current	The absolute maximum charge current, in amps.
Maximum Discharge Current	The absolute maximum discharge current, in amps.

8.4.2.2 Lifetime

For the Battery lifetime is limited by option, select the time, throughput, or time and throughput radio button (HOMER Pro, 2023b). If you select:

- Time, the storage unit requires replacement after a fixed length of time (float life, years).
- Throughput, the storage unit requires replacement after a fixed quantity of energy cycles through it (throughput, kWh).
- Time and Throughput, the storage unit requires replacement when the first of these two values are reached.

To establish a specific lifespan for the storage unit, you have two options in the HOMER software.

First, if you want to limit the storage life based on a certain number of years, you can input that duration as the "Float life" parameter.

Second, if you prefer to limit the storage life based on a specific quantity of energy throughput, you can enter that value as the "Lifetime throughput." Additionally, you have the option to select the "Enter lifetime curve" box, which aids in calculating the lifetime throughput value.

During a lifetime test, the storage unit undergoes a series of regular charge and discharge cycles under controlled conditions. Each cycle involves discharging the storage to a particular depth and then fully recharging it. The purpose of this test is to determine the number of such cycles the storage unit can endure before it requires replacement. Manufacturers conduct multiple tests at various depths of discharge to generate the storage unit's lifetime curve and ascertain the product's longevity (HOMER Pro, 2023b). The lifetime curve depicts the relationship between the number of cycles until failure and the depth of those cycles, as illustrated below (HOMER Pro, 2023b).

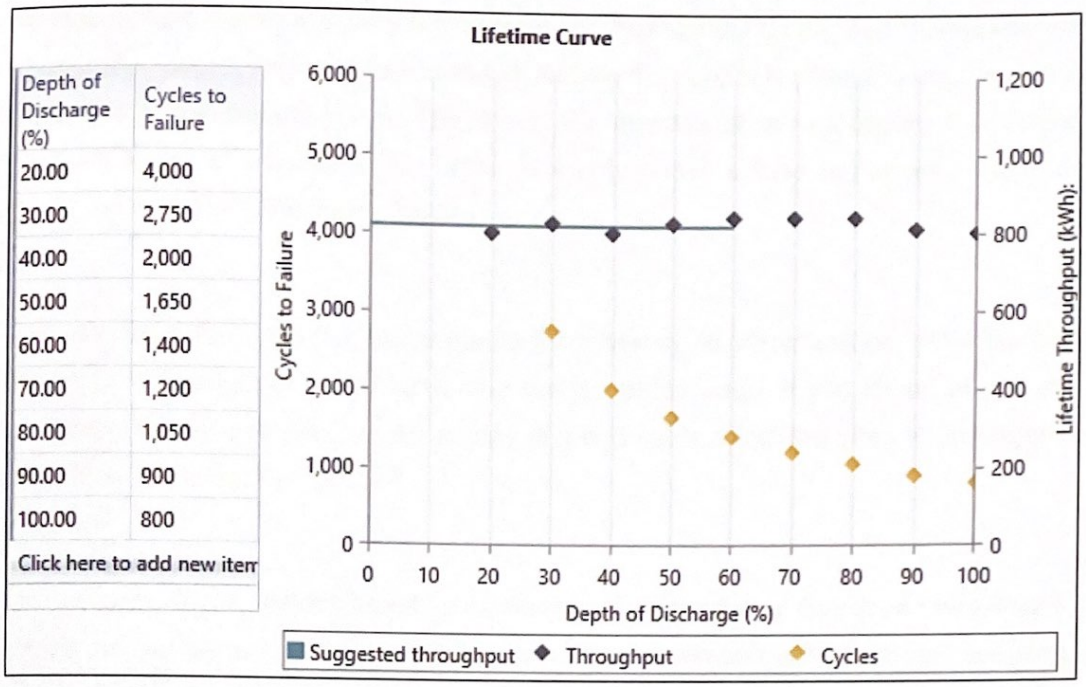

Figure 16: Battery lifetime curve

In HOMER, you can define the storage lifetime curve as a table of cycles to failure versus depth of discharge (HOMER Pro, 2023b). That set of points is represented by HOMER as yellow diamonds. That plot, like the one before, often indicates a rapid decrease in the number of cycles to failure as the depth of discharge increases (HOMER Pro, 2023b). HOMER also depicts lifetime throughput, which it computes for each point on the lifetime curve using the following equation (HOMER Pro, 2023b):

$$Q_{lifetime,i} = f_i d_i \left(\frac{q_{max} V_{nom}}{1000 W/kW} \right) \quad (4)$$

Where:

$Q_{lifetime,i}$ = the lifetime throughput [kWh]
f_i = the number of cycles to failure
d_i = the depth of discharge [%]
q_{max} = the maximum capacity of the storage [Ah]
V_{nom} = the nominal voltage of the storage [V]

HOMER displays these values as black diamonds on the lifetime curve (right y-axis). Their values typically indicate just a weak influence on discharge depth. HOMER's

simulation logic makes the simplistic assumption that lifetime throughput is independent of discharge depth. The calculated value of lifetime throughput is shown by the horizontal black line in the lifetime curve. The line is the average of the calculated throughput numbers for all of the points you enter. It is only drawn across the allowed depth of discharge range (HOMER Pro, 2023b).

The calculated lifetime throughput is merely for reference; in the simulation, HOMER uses the Lifetime throughput (kWh) input near the top of the page. If you intend to use the computed throughput value, make a copy of it and paste it into the Lifetime throughput (kWh) box (HOMER Pro, 2023b).

The battery characteristics studied for modeling include discharge rate dependent losses, temperature dependence on capacity, cycle lifetime estimation using rain-flow counting, and cycle by cycle deterioration based on discharge depth. The battery's minimum SOC is considered to be 20% (HOMER Pro, 2023b).

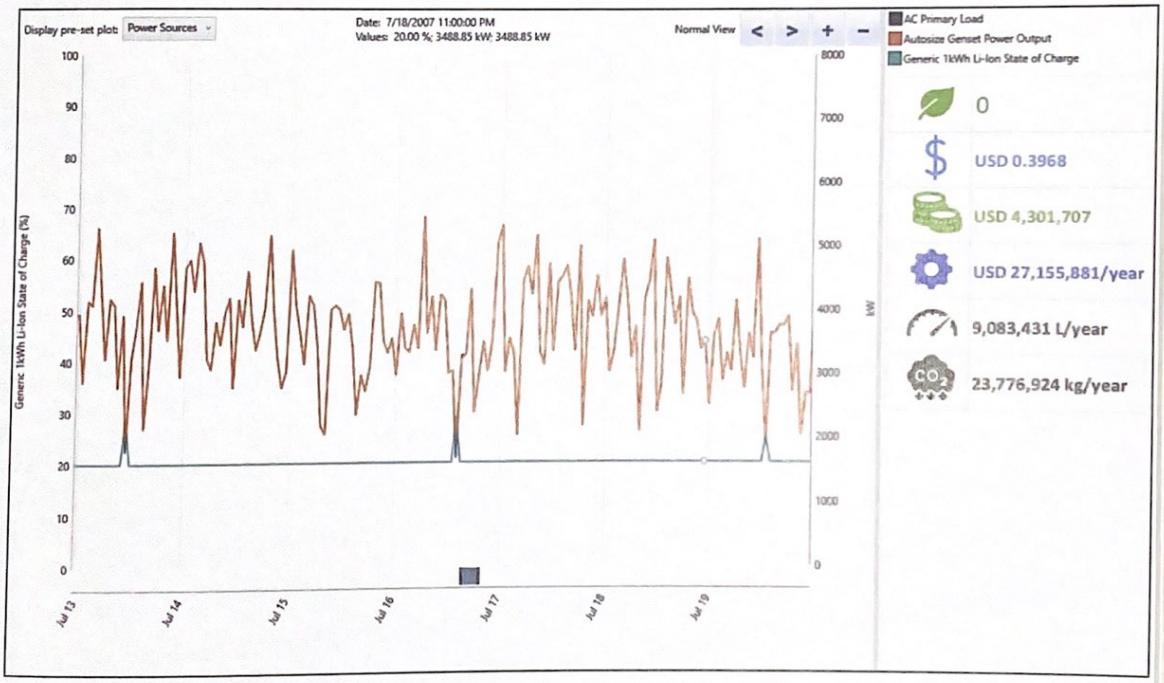

Figure 17: System Output Profile with Large DG + Energy Storage

From the simulation results, as shown in Figure 17, we can observe that the addition of a lithium-ion battery storage with a capacity of 609 kWh is not feasible.

This configuration will help to achieve reductions in fuel consumption and CO^2 emissions, but it will increase the overall O&M cost, resulting in a further increase in LCOE.

8.4.3 Large DG + Energy Storage + PV

The following equation have been utilized to find the output from the PV array.

$$P_{PV} = Y_{PV} f_{PV} \left(\frac{\overline{G}_T}{\overline{G}_{T,STC}} \right) \left[1 + \alpha_P \left(T_c - T_{c,STC} \right) \right] \quad (5)$$

where:

Y_{PV} = the rated capacity of the PV array, meaning its power output under standard test conditions [kW]

f_{PV} = the PV derating factor [%]

$\overline{G}_T$ = the solar radiation incident on the PV array in the current time step [kW/m^2]

$\overline{G}_{T,STC}$ = the incident radiation at standard test conditions [1 kW/m^2]

α_P = the temperature coefficient of power [%/°C]

T_c = the PV cell temperature in the current time step [°C]

$T_{c,STC}$ = the PV cell temperature under standard test conditions [25°C]

In this report's HelioScope and Homer Pro results, we examined the solar radiation profile, optimum tilt angle, and maximum PV (photovoltaic) capacity that can be put at the Bayankhundii Mine Site. The simulation was run to examine the system while taking these input values and temperature effects into account.

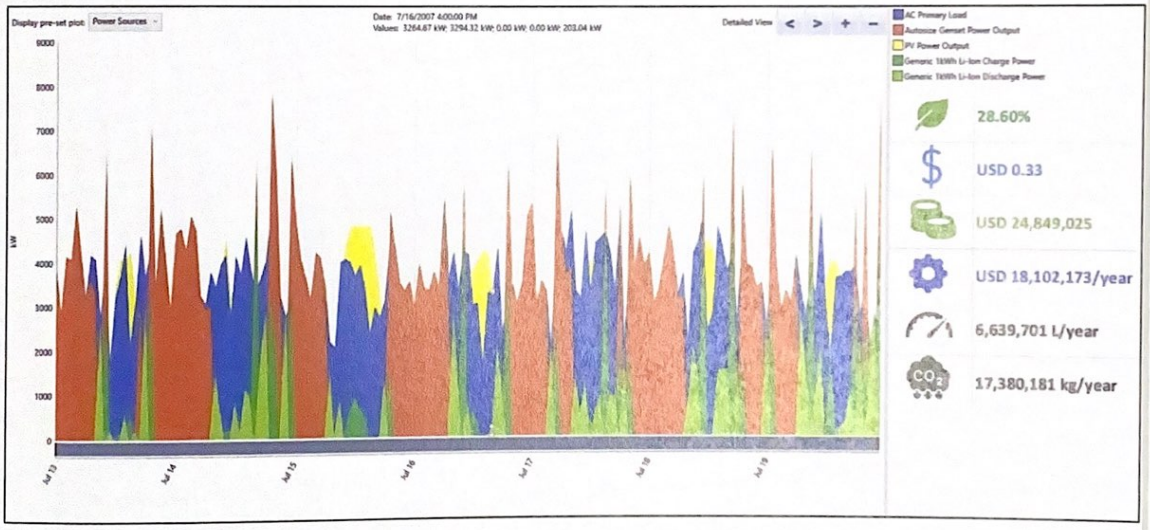

Figure 18: System Output Profile with Large DG + Energy Storage + PV

Adding a PV capacity of 6000 kW, we can observe that a renewable penetration of 28.6% can be achieved for our system. With this design, we need a storage capacity of 7313

kWh to store and efficiently use the excess solar energy available during the day. The installation of PV and energy storage has greatly raised the capital cost, but due to a large reduction in fuel consumption, we can expect a decrease in operational cost, leading to a further decrease in LCOE.

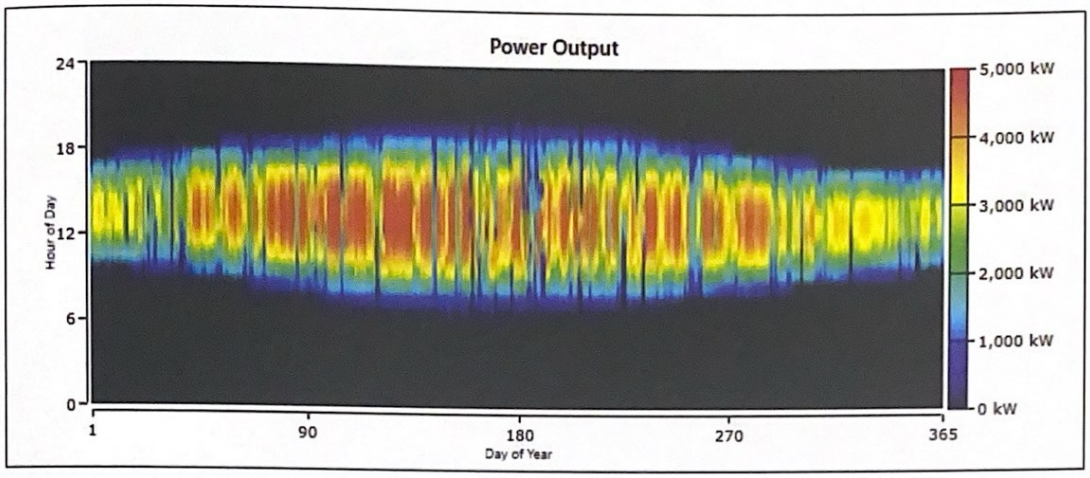

Figure 19: PV Power Output Figure

Figure 19 shows the output from PV. We can see that the maximum output is in the summer season, when the solar radiation is at its maximum, as we already analyzed in Figure 8: Daily Solar Radiation (Global Horizontal).

8.4.4 DG + Energy storage + PV + Wind energy

The following equation is used to calculate the wind speed at a hub height of wind turbine.

$$U_{hub} = U_{anem} \cdot \frac{\ln(z_{hub} / z_0)}{\ln(z_{anem} / z_0)} \quad (6)$$

where:

U_{hub} = the wind speed at the hub height of the wind turbine [m/s]
U_{anem} = the wind speed at anemometer height [m/s]
z_{hub} = the hub height of the wind turbine [m]
z_{anem} = the anemometer height [m]
z_0 = the surface roughness length [m]
ln(..) = the natural logarithm

The below equation is for the calculation of the wind turbine power output.

$$P_{WTG} = \left(\frac{\rho}{\rho_0} \right) \cdot P_{WTG,STP} \quad (7)$$

where:

P_{WTG} = the wind turbine power output [kW]
$P_{WTG,STP}$ = the wind turbine power output at standard temperature and pressure [kW]
ρ = the actual air density [kg/m^3]
ρ_0 = the air density at standard temperature and pressure (1.225 kg/m^3)

As a result of the wind profile and Weibull distribution analysis in Figure 9: Average Wind Velocity @ 50m Hub Height and Figure 10: Weibull Distribution Curve at Average Wind Speed of 6 m/s, it was evident that the Bayankhundii's average wind speed was 6.23 m/s at 50m hub height.

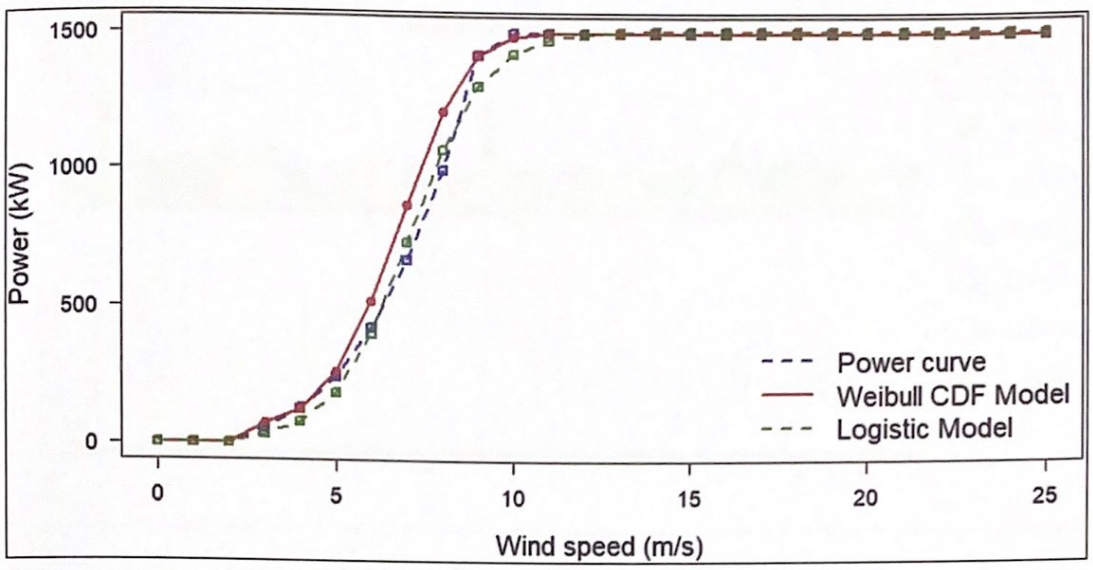

Figure 20: Power Curve of 1.5MW Wind Turbine

Power curves are commonly used to illustrate the performance of wind turbines under standard temperature and pressure (STP) conditions. In Figure 20, we present the power curve for a Generic 1.5MW model wind turbine. These results were derived from a wind test report conducted in accordance with AWEA Standard 9.1-2009.

The power curve provides valuable information about the turbine's power output at various wind speeds. For this particular wind turbine model, the rated power is 1.5MW, achieved at a wind speed of 11.4m/s. Additionally, the turbine has a cut-in wind speed of 3.5m/s, indicating the minimum wind speed required for it to start generating power.

By examining the power curve, we can observe that at an average wind speed of 6.23m/s, each turbine is capable of harnessing 400kW of energy from the wind. This information is essential for conducting simulation studies and making accurate assessments based on the provided wind parameters.

The simulation study referenced in your statement was conducted utilizing the specified wind parameters outlined above, enabling a comprehensive analysis of the wind turbine's performance under the given conditions.

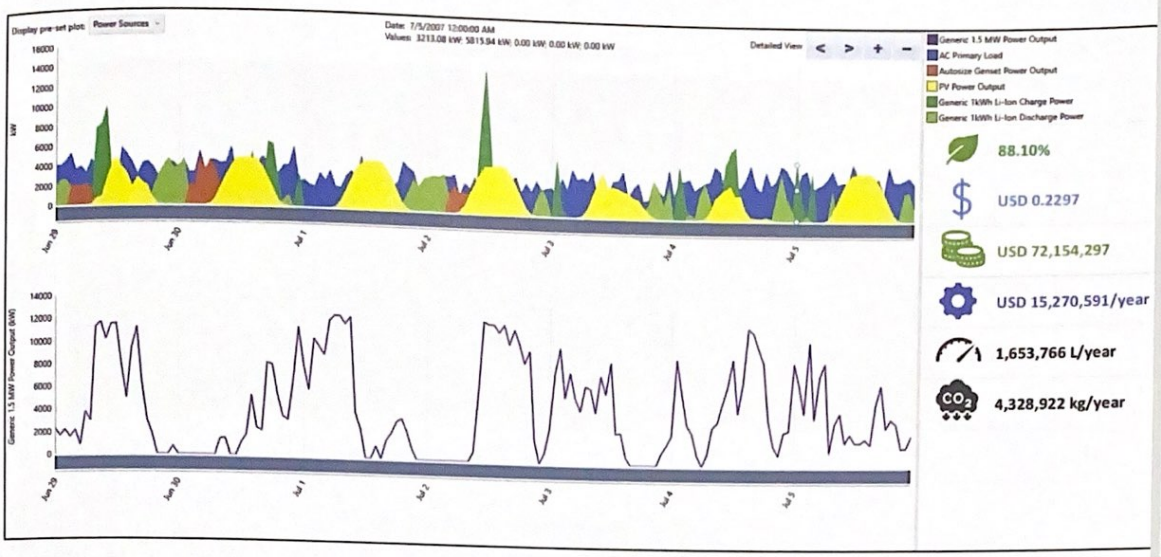

Figure 21: System Output Profile of Large DG + Energy Storage + PV + Wind Energy

Based on the simulation results, it is evident that a combination of a 6000 kW PV system and a 15,000-kW wind turbine requires a lithium-ion battery capacity of 38,196 kWh.

By incorporating these large wind turbines and energy storage systems, we were able to achieve a remarkable increase in renewable penetration, reaching 88.10%, while also reducing the levelized cost of electricity (LCOE) to the lowest compared with other configurations.

Nevertheless, it is important to note that the higher capital cost associated with the wind turbine is a factor to consider. Additionally, the fluctuation of wind power output can be observed in Figure 21 depicted above.

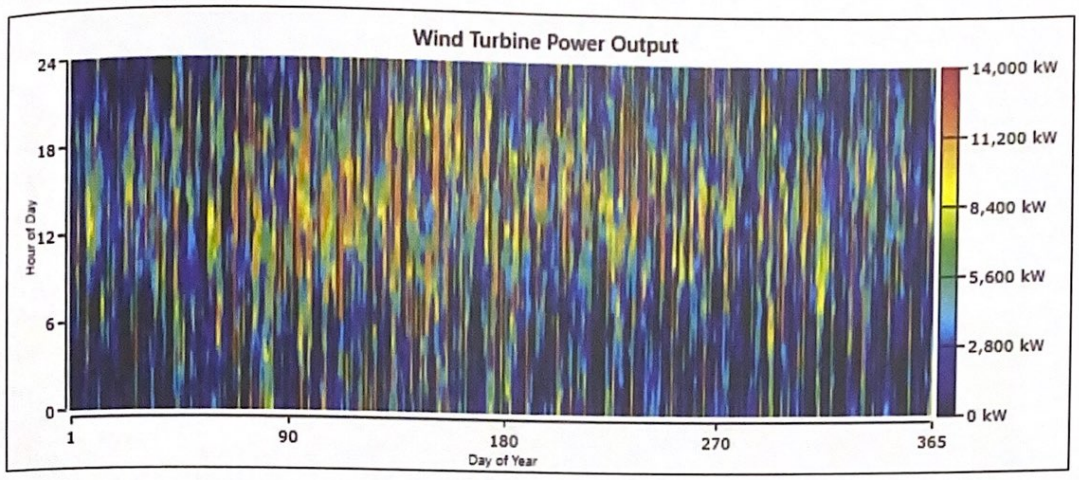

Figure 22: Wind Power Output

Based on the analysis presented in Figure 22, it is noticeable that the wind turbine output remains below 3,901 kW for the majority of the year. This outcome is primarily due to the relatively low average wind speed at the selected mine site.

As a consequence, the expected cost savings from the integration of the wind turbine were not substantial.

8.4.5 Summary for Off-Grid System

Table 5: Summary of Off-Grid System Analysis (on the following page) provides a comprehensive summary of the off-grid system analysis. Based on the summary, it can be inferred that the most feasible option is indicated by the blue-highlighted third column.

However, the cheapest combination was the green-highlighted fourth option is considered the optimal configuration for operating the Bayankhundii mine site entirely as an off-grid system. This configuration results in a yearly reduction of operating costs and CO^2 emissions by as much as 88.1% when compared to a system solely reliant on diesel generators.

However, it is important to note that the output from wind sources relies on the stochastic wind profile, requires further site survey to accurately measure the actual wind conditions.

Table 5: Summary of Off-Grid System Analysis

Icons	Large DG	DG + Storage	DG + Storage + PV	**DG + Storage + PV + Wind**	DG + Storage + Wind
	7900 kW	7900 kW	7900 kW	7900 kW	7900 kW
	N/A	609 kWh	7313 kWh	38196 kWh	36883 kWh
	N/A	N/A	6000 kW	6000 kW	N/A
	N/A	N/A	N/A	15000 kW (1.5MW x 10 pcs)	21000 kW (1.5MW x 14 pcs)
	0%	0%	28.60%	88.10%	86.6%
	$0.3959	$0.3968	$0.33	$0.2297	$0.24
	$3,950,000	$4,301,707	$24,849,025	$72,154,297	$68,299,145.65
	$27,076,456/yr.	$27,155,881/yr.	$18,102,173/yr.	$15,270,591/yr.	$18,002,742.32
	9,084,773 L/yr.	9,083,431 L/yr.	6,639,701 L/year	1,653,766 L/yr.	2,032,151 L/yr.
	23,780,438 kg/yr.	23,776,924kg/yr.	17,380,181 kg/yr.	4,328,922 kg/yr.	5,319,388 kg/yr.
	-	-	6.46 yrs.	6.5 yrs.	7.4 yrs.

9 Business Case

9.1 Business Canvas Model

Alexander Osterwalder first proposed the Business Model Canvas and it is a tool for visualizing and documenting existing business models (Denim, 2017). Using this canvas, you will gain insights into numerous categories such as value proposition, important activities, customer segmentation, and revenue streams (Denim, 2017).

Only a few segments relevant to my master's thesis will be discussed in the following sections.

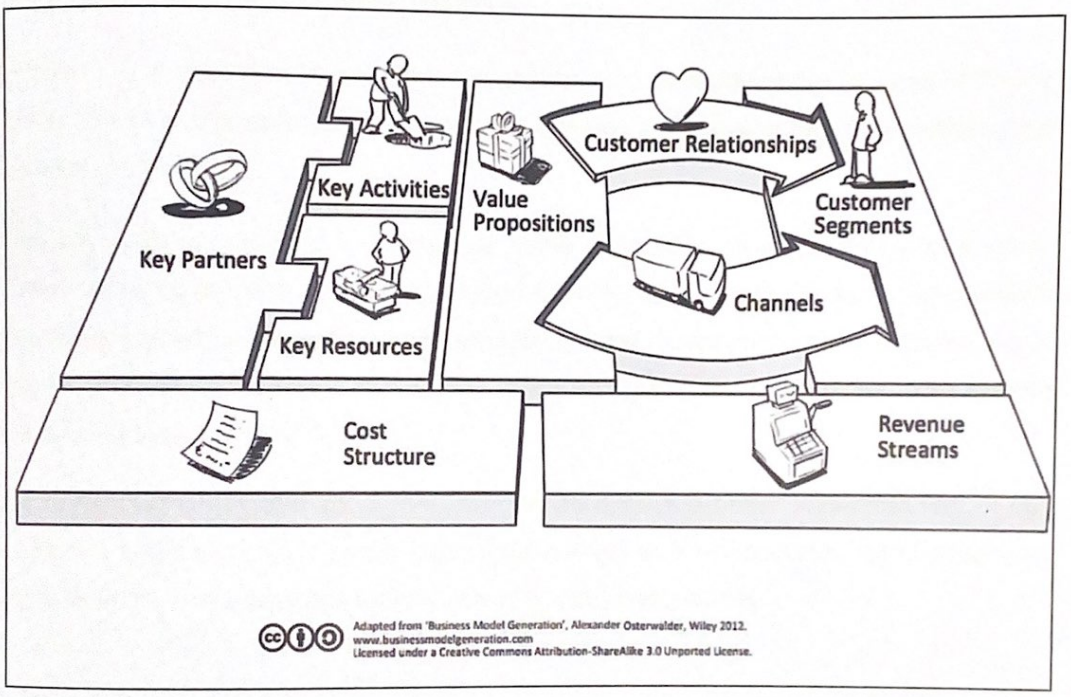

Figure 23:Business Canvas Model (Osterwalder & Pigneur, 2013).

Customer segments refer to the specific groups of customers for whom we create value. In the case of Mongolia, our customer segments include all the mines located in Southwest Mongolia, including the Bayankhundii mining site. These mines either rely on diesel generators due to an inconsistent power grid or operate completely off-grid.

The core of our business model lies in the value proposition, which encompasses the products, services, or solutions that provide significant benefits to our customers. Our value proposition revolves around minimizing the operational costs of the existing diesel-powered systems by implementing a hybrid renewable energy system. By doing so, we not only reduce their expenses but also contribute to a substantial decrease in CO2 emissions.

To ensure the successful execution of the project, establishing key partnerships is crucial. These partnerships may involve collaborating with research institutions, consulting companies, and other relevant stakeholders. In our pursuit, we have conducted thorough market research and held regular meetings with major suppliers to identify suitable equipment providers for various components such as photovoltaic (PV) systems, control mechanisms, and energy storage solutions.

However, it is important to note that Bayankhundii is currently in the process of finding collaborators and suppliers, actively working towards establishing essential relationships with key partners.

The key activities required to deliver our value proposition involve a range of actions. These activities include conducting comprehensive site surveys, carrying out detailed feasibility studies, performing both basic and detailed engineering tasks, participating in tender processes, managing system operation and maintenance, implementing remote monitoring systems, and more.

By enhancing clarity and coherence, we aim to ensure a better understanding of our customer segments, value proposition, partnerships, and key activities, all of which are integral to the successful implementation of our business model.

9.2 Cost Parameters Definition

The cost parameters that I evaluated in my study are listed below.

- Levelized Cost of Energy (LCOE): It is the average cost per kWh of the useful electrical energy produced by the system.

$$LCOE = \frac{C_{ann,tot}}{E_{served}} \tag{8}$$

Where,

$C_{ann,tot}$ = total annualized cost of the system [USD/year]

E_{served} = total electrical load served [kWh/year]

- Nominal Discount/Interest Rate (i'): The rate at which one can borrow money (%).
- Real Discount Rate (i): The real discount rate is used to convert between one-time costs and annualized costs.

$$i = \frac{i' - f}{1 + f} \tag{9}$$

Where:

i = real discount rate

i' = nominal discount rate

f = expected inflation rate

- Net Present Cost (NPC): The net present cost of a component is calculated by summing the present values of all installation and operating costs and then subtracting the present values of all revenues generated throughout the project's lifetime. This calculation takes into account the time value of money, allowing for a fair assessment of the component's costs and revenues in today's terms.

- Present Value (PRV): Taking into account the time value of money, the present value is the current equivalent value of a set of future cash flows.

$$PRV = \frac{CF}{(1+i)^N} \quad (10)$$

Where:

CF = future cash flows

i = the annual real discount rate [%]

N= number of years

- Annualized Cost (C_{ann}): The annualized cost of a component refers to the cost that, if distributed equally over each year of the project's lifetime, would result in the same net present cost as the actual cost distribution (Denim, 2017). It represents the annual expense associated with owning, operating, and maintaining an asset throughout its entire lifespan (Denim, 2017). This concept allows for a simplified assessment of the component's cost structure on an annual basis, providing a useful metric for budgeting and financial planning purposes (Denim, 2017).

$$C_{ann} = \mathrm{CRF}\left(i, R_{proj}\right) \cdot C_{NPC} \quad (11)$$

Where,

C_{NPC} = the net present cost [USD]

i = the annual real discount rate [%]

R_{Proj} = the project lifetime [years]

CRF = the capital recovery factor

- Capital Recovery Factor (CRF): The ratio used to determine the present value of the annuity is known as capital recovery factor.

$$CRF(i,N) = \frac{i.(1+i^N)}{(1+i^N)-1} \quad (12)$$

Where,

i = real discount rate

N= number of years

- Sinking Fund Factor (SFF): The ratio used to determine the future value of a series of equal cash flow.

$$SFF(i,N) = \frac{i}{(1+i^N)-1} \quad (13)$$

- Salvage Value (S): Salvage value is the value remaining in a component of the power system at the end of the project lifetime.

$$S = C_{rep} \cdot \frac{R_{rem}}{R_{com}} \quad (14)$$

Where,

C_{rep} = replacement cost [USD]

R_{rem}= remaining life of component at the end of the project lifetime

R_{com} = component lifetime

- Operating Cost ($C_{operating}$): The operating cost is the annualized value of all costs and revenues other than initial capital costs.

$$C_{operating} = C_{ann,tot} - C_{ann,cap} \quad (15)$$

Where,

$C_{ann,tot}$ = the total annualized cost [USD/year]

$C_{ann,cap}$ = the total annualized capital cost [USD/year]

- ROI (Return on Investment): ROI is the rate of return on, i.e., cost saving achieved yearly on money invested. It is calculated using the equation below.

$$ROI = \frac{\sum_{i=0}^{R_{proj}} C_{i,ref} - C_i}{R_{proj}\left(C_{cap} - C_{cap,ref}\right)} \quad (15)$$

where:

$C_{i,ref}$ = nominal annual cash flow for base (reference) system

C_i = nominal annual cash flow for current system

R_{proj} = project lifetime in years

C_{cap} = capital cost of the current system

$C_{cap,ref}$ = capital cost of the base (reference) system

10 Business Case for Bayankhundii Mine Site

Table 8 the next page displays the summary of three different off-grid configurations to develop a business case.

The first column indicates the first configuration with typical systems at remote mines in Mongolia running with diesel generators only.

The second column indicates the second configuration with 7.9 MW diesel generators + 6 MW PV + 7.3 MWh energy storage.

And, the third and last column indicate the third configuration with the same 7.9 MW diesel generators + 6 MW PV + 15 MW wind and 38.1 MWh energy storage.

All the systems are not connected to the grid, therefore relying completely on their own energy production. Below,

Table 6 summarizes the 1st and 3rd configuration cost summaries, and

Table 7 demonstrates the economical results of the 3rd configuration as compared to the 1st configuration.

Table 6: Cost Summary

	Base case	Lowest cost system
NPC	$176M	$102M
Initial Capital	$3.95M	$72.2M
O & M	$13.2M/yr	$2.32M/yr
LCOE	$0.396/kWh	$0.230/kWh

Table 7: Economics of Winning System

Metric	Value
Present worth ($)	$74,039,220
Annual worth ($/yr)	$5,677,047
Return on investment (%)	9.5
Internal rate of return (%)	12.8
Simple payback (yr)	6.52
Discounted payback (yr)	6.93

Table 8: Summary of Off-Grid Systems with Pie Chart

Icons	Large DG (First configuration)	DG + Storage + PV (Second configuration)	**DG + Storage + PV + Wind (Third configuration)**
PIE CHART	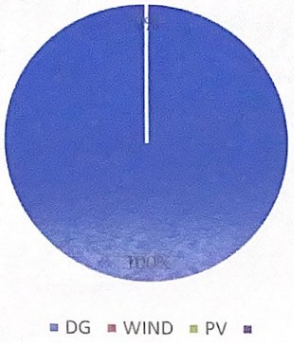	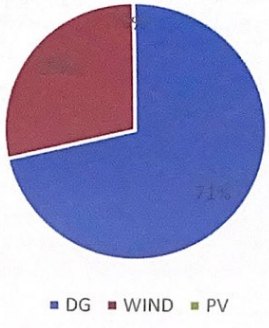	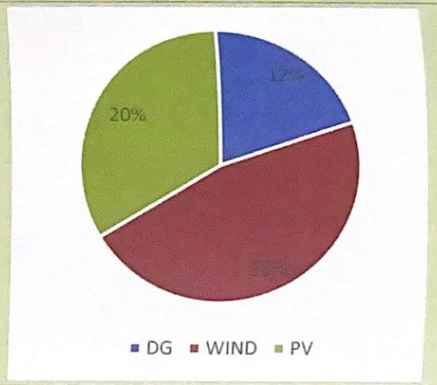
	7900 kW	7900 kW	7900 kW
	N/A	7313 kWh	38196 kWh
	N/A	6000 kW	6000 kW
	N/A	N/A	15000 kW (1.5MW x 10 pcs)
	0%	28.60%	88.10%
	$0.3959	$0.33	$0.2297
	$3,950,000	$24,849,025	$72,154,297

	$27,076,456/yr.	$18,102,173/yr.	$15,270,591/yr.
	9,084,773 L/yr.	6,639,701 L/year	1,653,766 L/yr.
	23,780,438 kg/yr.	17,380,181 kg/yr.	4,328,922 kg/yr.
	-	6.46 yrs.	6.5 yrs.

10.1.1 Cash Flow

Cash flow is the entire amount of money going into and out of a business (Denim, 2017).

Figure 24 and Figure 25 display the nominal cash flow by cost type and component type for the optimum hybrid system solution previously mentioned.

Figure 24 and Figure 25 show that adding Large DG, wind, PV, energy storage, and a system converter or controller requires a high initial capital cost of USD 72,154,297 during the first year. The running costs include maintenance and a very tiny percentage for diesel fuel. We incur replacement costs for DG and storage, which have a shorter lifetime than other components in the energy mix, during the eighth year period.

At the end of the project's life cycle, we may see some salvage value supplied by components such as the battery and system converter, both of which have a five-year remaining lifetime. Generator salvage value is negligible.

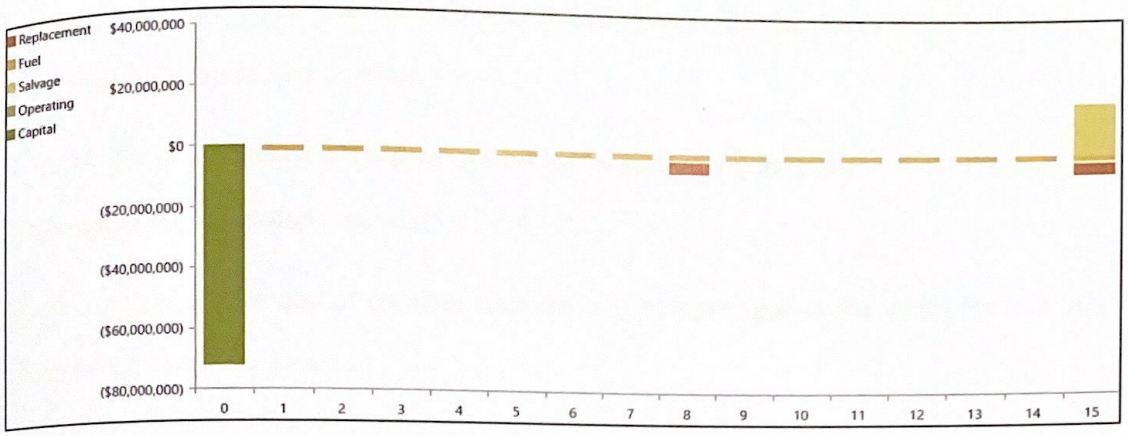

Figure 24: Nominal Cash Flow by Cost Type

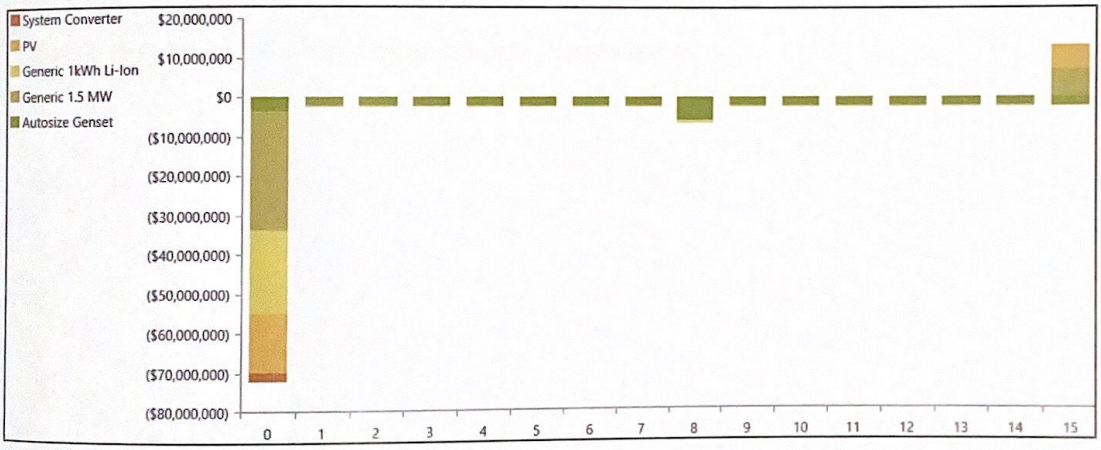

Figure 25: Nominal Cash Flow by Component Type

10.1.2 Pay Back Period

The payback period is amount of time required to recover the capital or initial investment, and it is usually measured in years.

In our analysis, we calculate the payback period by comparing the off-grid hybrid renewable system with the generator-only system.

Figure 26 displays the plot of nominal cumulative cash flow against the years for both the hybrid and diesel-only systems.

As we can observe that the large DG system requires significantly lower initial capital investment, resulting in a lower nominal cumulative cash flow compared to the hybrid system initially.

However, at a payback period of 6.5 years, the cash flow of the hybrid system starts to become lower than that of the other system. We also calculated the discounted payback period, taking into account the discount rate mentioned in

Table 2, which is determined to be as low as 6.93 years, as indicated in Table 7: Economics of Winning System.

Furthermore, the analysis reveals that the net present cost (NPC) amounts to 176 million USD, the return on investment (ROI) stands at 9.5%, and the internal rate of return (IRR) is estimated to be 12.8%.

In our case, the ROI falls below the average, indicating a relatively lower return on the investment. However, the payback period is short compared to similar projects, suggesting a quicker recovery of the initial investment.

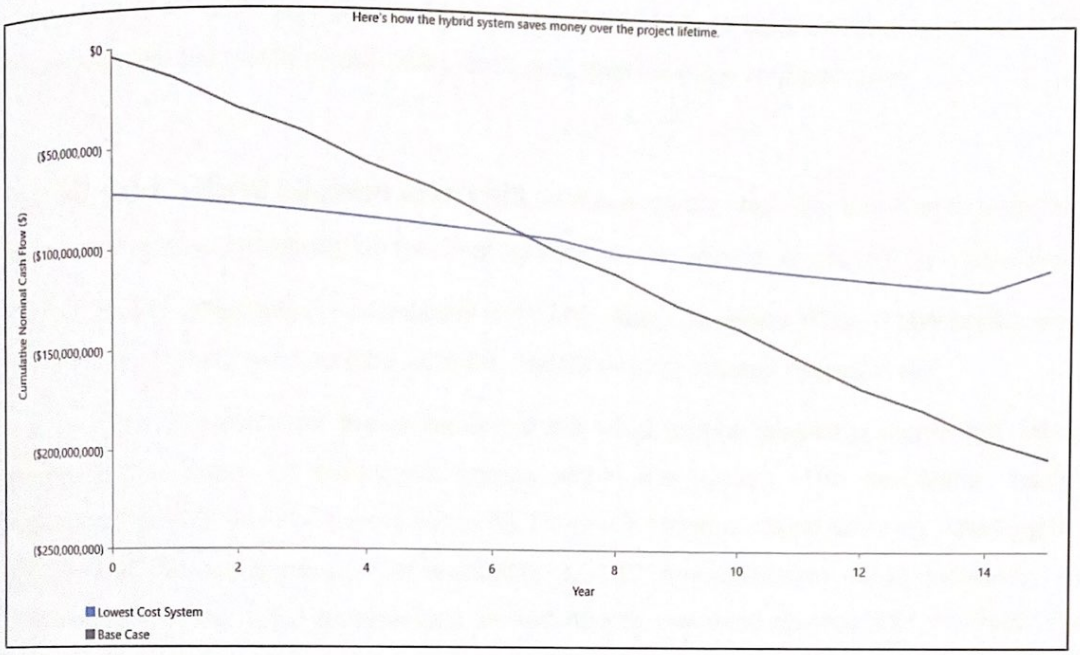

Figure 26: Nominal Cumulative Cash Flows

11 Conclusion

The main objective of this thesis was to develop conceptual designs for off-grid systems that can effectively meet the energy requirements of mining companies in the southwestern region of Mongolia in an energy-efficient, reliable, and environmentally sustainable solution. Additionally, market research was conducted to identify key equipment suppliers for the Bayankhundii off-grid microgrid systems, considering factors such as modularity, reliability, robustness, performance guarantees, cost, and maintenance requirements.

For off-grid hybrid system analysis, in this analysis, the objective was to determine the optimal system configuration for an off-grid scenario; without access to the national grid.

The proposed configuration consisted of a 7.9 MW diesel generator (DG), 6 MW photovoltaic (PV) panels, 15 MW wind turbine, and 38.1 MWh energy storage respectively.

The findings revealed that the inclusion of the wind turbine played a significant role in increasing the share of renewable energy within the system. The renewable fraction increased from 28.6% (PV + storage) to 88.1% (PV + storage + wind turbine), resulting in a reduction in the levelized cost of electricity (LCOE) and operating costs. However, the effectiveness of the wind turbine was limited due to low wind speeds and the high cost associated with taller hub heights (>50m). The output of the wind turbine is heavily influenced by the wind velocity, which has stochastic characteristics and can be affected by factors such as water discharge from upstream. Therefore, accurate prediction of output and cost savings would require in situ measurements and analysis prior to implementing such technologies.

On the other hand, PV panels can be installed with any tilt angle, eliminating the need to avoid inter-row shading and allowing for a peak capacity of 6 MW. Their performance is not as reliant on external factors as wind turbines, making them a more predictable and consistent energy source.

The analysis demonstrated that a hybrid system incorporating PV, wind, and energy storage can significantly increase the share of renewable energy and reduce costs in an off-grid mining scenario.

However, the implementation of wind turbines requires careful consideration of site-specific factors, such as wind speed and cost-effectiveness, while PV panels offer greater flexibility and reliability in energy generation.

12 Outlook and Future works

It is important to acknowledge that the optimal configuration mentioned above is not a universal solution applicable to all mines in Mongolia, as individual analysis is required based on factors such as project location, load profile, equipment usage patterns, fuel prices, and project lifespan. Furthermore, advancements in technology and ongoing research may lead to changes in the optimal configuration in the future.

Accurate prediction of yearly load escalation or fluctuation is critical in determining the most suitable solution. Developing algorithms that utilize machine learning and artificial intelligence can improve the accuracy of load profile predictions. This enables a more precise assessment of the optimal system configuration.

Additionally, it is essential to consider that simulation output parameters, including capital cost, operating cost, and payback period, are subject to change based on input technical parameters and the costs associated with various technologies, which can be influenced by market price fluctuations.

In summary, the optimal configuration for off-grid mining systems is not static and must be evaluated on a case-by-case basis, considering specific project characteristics. Accurate load prediction, the development of advanced algorithms, and an understanding of the variability of simulation output parameters are crucial for making informed decisions and adapting to evolving technologies and market conditions.

List of Abbreviations and Acronyms

AC Alternating Current

BMS Battery Management System

CHP Combined Heat and Power

DC Direct Current

DCS Distributed Control Systems

DERs Distributed Energy Resources

DG Diesel Generator

EMS Energy Management Systems

GCR Ground Clearance Ratio

GHG Greenhouse Gas Emissions

Hz Hertz

IEC International Electrotechnical Commission

IRR Internal Rate of Return

kW Kilowatt

kWh Kilowatt Hours

kWp Kilowatt Peak

LCOE Levelized Cost of Electricity

NPC Net Present Cost

NREL National Renewable Energy Laboratory

O&M Operation and Maintenance

PCS Power Conversion System

PMS Power Management System

PV Photovoltaic

RESs Renewable Energy Systems

ROI Return on Investment

SCADA Supervisory Control and Data Acquisition

SOC State of Charge

UNDP United Nations Development Programme

Bibliography

1. CAT. (2023, May 28). *The Impact Of Generator Set Underloading | Cat | Caterpillar*. Https://Www.Cat.Com/En_US/by-Industry/Electric-Power/Articles/White-Papers/the-Impact-of-Generator-Set-Underloading.Html. https://www.cat.com/en_US/by-industry/electric-power/Articles/White-papers/the-impact-of-generator-set-underloading.html
2. Denim, D. (2017). *Design and Analysis of a Hybrid Renewable Microgrid System for Humanitarian Help*.
3. Ellabban, O., & Alassi, A. (2021). Optimal hybrid microgrid sizing framework for the mining industry with three case studies from Australia. *IET Renewable Power Generation*, *15*(2), 409–423. https://doi.org/10.1049/rpg2.12038
4. Gómez, J. S., Rodriguez, J., Garcia, C., Tarisciotti, L., Flores-Bahamonde, F., Pereda, J., Nuñez, F., Cipriano, A. Z., & Salas, J. C. (2020). An Overview of Microgrids Challenges in the Mining Industry. *IEEE Access*, *8*, 191378–191393. https://doi.org/10.1109/ACCESS.2020.3032281
5. Hirsch, A., Parag, Y., & Guerrero, J. (2018). Microgrids: A review of technologies, key drivers, and outstanding issues. *Renewable and Sustainable Energy Reviews*, *90*, 402–411. https://doi.org/10.1016/j.rser.2018.03.040
6. HOMER Pro. (2023a, May 28). *How HOMER Creates the Generator Efficiency Curve*. HOMER Pro 3.9. https://www.homerenergy.com/products/pro/docs/3.9/how_homer_creates_the_generator_efficiency_curve.html
7. HOMER Pro. (2023b, May 28). *Optimize the value of your hybrid power system-from utility-scale and distributed generation to standalone microgrids*. HOMER. https://www.homerenergy.com/
8. IEA. (2023, May 28). *Total energy supply (TES) by source, Mongolia 1990-2020*. IEA. https://www.iea.org/countries/mongolia
9. James, K. (2022, March). *Gold Fields Agnew Gold Mine Final Report*. Australian Renewable Energy Agency. https://arena.gov.au/knowledge-bank/gold-fields-agnew-gold-mine-final-report/
10. Kim, J.-Y., Park, J. H., & Lee, H.-J. (2011). Coordinated Control Strategy for Microgrid in Grid-Connected and Islanded Operation. *IFAC Proceedings Volumes*, *44*(1), 14766–14771. https://doi.org/10.3182/20110828-6-IT-1002.01266

11. Media, 247Solar. (2021, December 2). Mining the Pathway to 100% Clean Power. *247Solar, Inc.* https://247solar.com/mining-case-study-pathway-100-percent-clean-power/
12. Microgrid Institute. (2020, May 28). *Microgrid Institute*. Microgrid Institute. http://www.microgridinstitute.org/
13. Mongolbank. (2023, May 28). *The Central Bank of Mongolia*. The Central Bank of Mongolia. https://www.mongolbank.mn/en
14. NREC. (2023, May 28). *Law of Monglia on Renewable Energy*. National Renewable Energy Center. https://www.nrec.mn/en/
15. Osterwalder, A., & Pigneur, Y. (2013). *Business Model Generation: A Handbook for Visionaries, Game Changers, and Challengers*. John Wiley & Sons.
16. Page, J. (2018). Chapter II-1-A - The Role of Solar-Radiation Climatology in the Design of Photovoltaic Systems. In S. A. Kalogirou (Ed.), *McEvoy's Handbook of Photovoltaics (Third Edition)* (pp. 601–670). Academic Press. https://doi.org/10.1016/B978-0-12-809921-6.00016-1
17. Paolo, N., & Kevin, H. (2017). *Insight Brief Toward Sustainable Mining*.
18. Pollack, K., & Bongaerts, J. C. (2020). Mathematical model on the integration of renewable energy in the mining industry. *International Journal of Energy Sector Management*, *14*(1), 229–247. https://doi.org/10.1108/IJESM-12-2018-0006
19. Rezkallah, M., Chandra, A., Singh, B., & Singh, S. (2019). Microgrid: Configurations, Control and Applications. *IEEE Transactions on Smart Grid*, *10*(2), 1290–1302. https://doi.org/10.1109/TSG.2017.2762349
20. ROMA. (2020). *Bayan Khundii Gold Project Feasibility Study* (Technical NI 43-101; p. 302). ROMA OIL AND MINING ASSOCIATES LIMITED. https://erdene.com/en/projects/bayan-khundii/
21. Saranchimeg, S., Sanjari, M. J., & Nair, N. K. C. (2018). Toward a Resilient Network by Optimal Sizing of Large Scale PV Power Plant in Microgrid-Case Study of Mongolia. *2018 Australasian Universities Power Engineering Conference (AUPEC)*, 1–5. https://doi.org/10.1109/AUPEC.2018.8757877
22. UNDP. (2013, August 2). *UNDP Global Annual Report 2013 | United Nations Development Programme*. UNDP. https://www.undp.org/mongolia/publications/undp-global-annual-report-2013
23. World Bank. (2017). *Toward a sustainable energy future for all: Directions for the World Bank Group' 's energy sector : Toward a sustainable energy future for all : directions for*

the World Bank Group's energy sector [Text/HTML]. World Bank. https://documents.worldbank.org/en/publication/documents-reports/documentdetail/745601468160524040/Toward-a-sustainable-energy-future-for-all-directions-for-the-World-Bank-Groups-energy-sector

24. Zhou, X., Guo, T., & Ma, Y. (2015). An overview on microgrid technology. *2015 IEEE International Conference on Mechatronics and Automation (ICMA)*, 76–81. https://doi.org/10.1109/ICMA.2015.7237460
25. Microgrid Institute. (2021). Microgrid Institute Framework. Retrieved from http://www.microgridinstitute.org/
26. National Renewable Energy Center of Mongolia. (2021). Laws and Regulations. Retrieved from http://www.nrec.mn/en/laws
27. World Bank. (2019). Mongolia Renewable Energy Sector Assessment. Retrieved from World Bank Group - International Development, Poverty, & Sustainability
28. Osterwalder, Y. Pigneur and T. Clark, Business model generation, Hoboken, N.J.: John Wiley & Sons, 2010.
29. Baker, Angela & Heiler, K & Ferguson, Sally. (2002). The effects of a roster schedule change from 8- to 12-hour shifts on health and safety in a mining operation. Journal of human ergology. 30. 65-70.

Appendix

Appendix 1:

Hi-MO 4m

LR4-72HPH 445~465M

21.4%	0~3%	<2%	0.55%	HALF-CELL
MAX MODULE EFFICIENCY	POWER TOLERANCE	FIRST YEAR POWER DEGRADATION	YEAR 2-25 POWER DEGRADATION	Lower operating temperature

Additional Value

25-Year Power Warranty

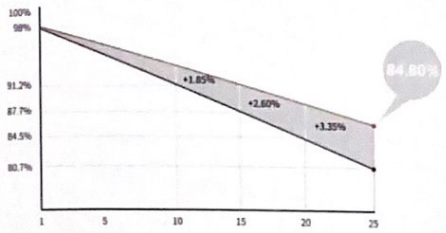

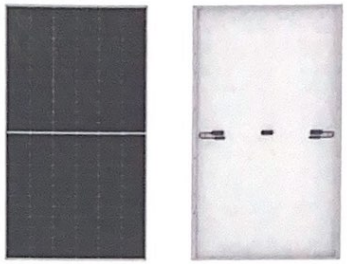

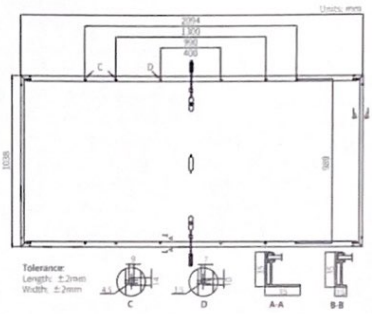

Mechanical Parameters

Cell Orientation	144 (6 × 24)
Junction Box	IP68, three diodes
Output Cable	4mm², +400, -200mm/±1400mm length can be customized
Glass	Single glass, 3.2mm coated tempered glass
Frame	Anodized aluminum alloy frame
Weight	24.3kg
Dimension	2094 × 1038 × 35mm
Packaging	30pcs per pallet / 150pcs per 20' GP / 660pcs per 40' HC

Electrical Characteristics

STC : AM1.5 1000W/m² 25°C NOCT : AM1.5 800W/m² 20°C 1m/s Test uncertainty for Pmax: ±3%

Module Type	LR4-72HPH-445M		LR4-72HPH-450M		LR4-72HPH-455M		LR4-72HPH-460M		LR4-72HPH-465M	
Testing Condition	STC	NOCT	STC	NOCT	STC	NOCT	STC	NOCT	STC	NOCT
Maximum Power (Pmax/W)	445	334.3	450	338.0	455	341.8	460	345.5	465	349.3
Open Circuit Voltage (Voc/V)	49.1	46.2	49.3	46.4	49.5	46.5	49.7	46.7	49.9	46.9
Short Circuit Current (Isc/A)	11.53	9.33	11.60	9.41	11.66	9.46	11.73	9.51	11.79	9.56
Voltage at Maximum Power (Vmp/V)	41.3	38.4	41.5	38.6	41.7	38.8	41.9	39.0	42.1	39.2
Current at Maximum Power (Imp/A)	10.78	8.70	10.85	8.75	10.92	8.81	10.98	8.86	11.05	8.91
Module Efficiency(%)	20.5		20.7		20.9		21.2		21.4	

Operating Parameters

Operational Temperature	-40°C ~ +85°C
Power Output Tolerance	0 ~ 3%
Voc and Isc Tolerance	±3%
Maximum System Voltage	DC1500V (IEC/UL)
Maximum Series Fuse Rating	20A
Nominal Operating Cell Temperature	45±2°C
Protection Class	Class II
Fire Rating	UL type 1 or 2 IEC Class C

Mechanical Loading

Front Side Maximum Static Loading	5400Pa
Rear Side Maximum Static Loading	2400Pa
Hailstone Test	25mm Hailstone at the speed of 23m/s

Temperature Ratings (STC)

Temperature Coefficient of Isc	+0.050%/°C
Temperature Coefficient of Voc	-0.265%/°C
Temperature Coefficient of Pmax	-0.340%/°C

LONGi

No.8369 Shangyuan Road, Xi'an Economic And Technological Development Zone, Xi'an, Shaanxi, China
Web: www.longi.com

Specifications included in this datasheet are subject to change without notice. LONGi reserves the right of final interpretation. (20220410V15)

Appendix 1.1: Solar Panel Technical Datasheet

GE Energy

1.5MW
Wind Turbine

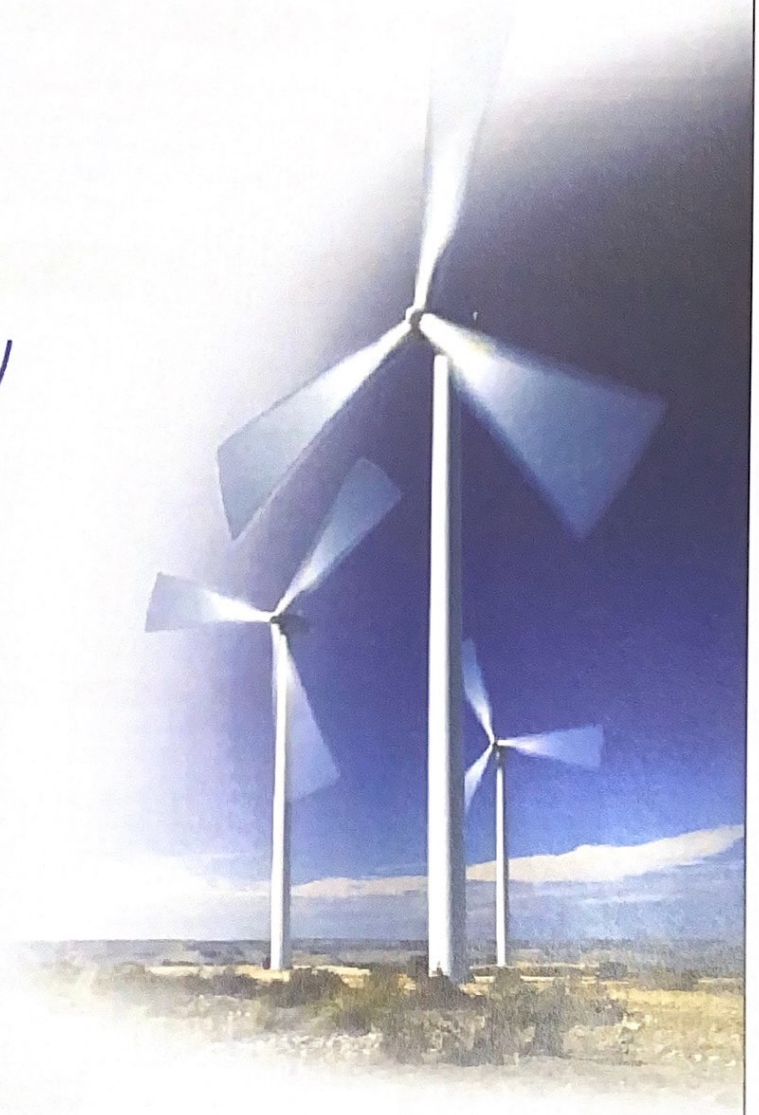

imagination at work

a product of
ecomagination

Advancing wind capture performance

As a leading global provider of energy products and services, GE continues to invest in advancing its 1.5 MW wind turbine product platform. With a core focus on enhancing efficiency, reliability, site flexibility and delivering multi-generational product advancements, GE's 1.5 MW wind turbine is the most widely used turbine in its class. Our commitment is to fully understand our customer's needs and respond with new technology enhancements aimed at capturing maximum wind energy to deliver additional return on investment.

Technical data

Operating Data		1.5sle	1.5xle
Rated Capacity:		1,500 kW	1,500 kW
Temperature Range: (with Cold Weather Extreme Package)	Operation:	-30°C – +40°C	-30°C – +40°C
	Survival:	-40°C – +50°C	-40°C – +50°C
Cut-in Wind Speed:		3.5 m/s	3.5 m/s
Cut-out Wind Speed (10 min avg.):		25 m/s	20 m/s
Rated Wind Speed:		14 m/s	11.5 m/s
Wind Class – IEC:		IIa V_{ref50} = 55 m/s V_{ave} = 8.5 m/s	IIIb V_{ref50} = 52.5 m/s V_{ave} = 8.0 m/s
Electrical Interface			
Frequency:		50/60 Hz	50/60 Hz
Voltage:		690V	690V
Rotor			
Rotor Diameter:		77 m	82.5 m
Swept Area:		4657 m²	5346 m²
Tower			
Hub Heights:		65/80 m	80 m
Power Control:		Active Blade Pitch Control	Active Blade Pitch Control

Power curve

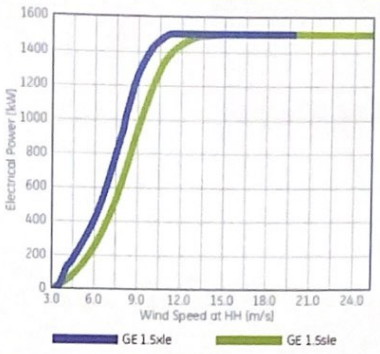

1.5sle – *Classic workhorse, an efficient and reliable machine with proven technology*
1.5xle – *Built on the success of the 1.5sle platform, captures more wind energy with 15% greater swept area*

GE's 1.5 MW wind turbine is designed to maximize customer value by providing proven performance and reliability. GE's commitment to customer satisfaction drives our continuous investment in the evolution of the 1.5 MW wind turbine through technological enhancements.

Evolution of the 1.5 MW

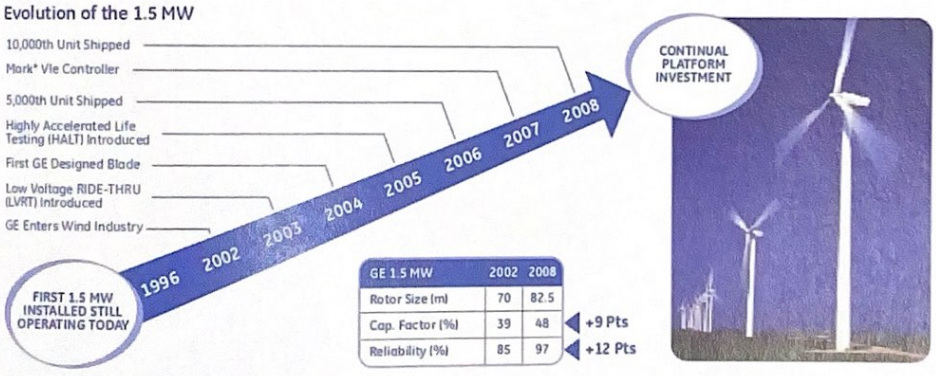

GE 1.5 MW	2002	2008	
Rotor Size (m)	70	82.5	
Cap. Factor (%)	39	48	+9 Pts
Reliability (%)	85	97	+12 Pts

Leading reliability and availability perform

GE's 1.5 MW wind turbine and services are designed to set the industry standard for product reliability and availability performance. GE's continual investments in technology, established infrastructure, research capabilities and globally recognized business processes allow GE to create and deliver customer value by maximizing energy capture and return on investment. This is evident through our model year performance trend where availability performance significantly improves each year.

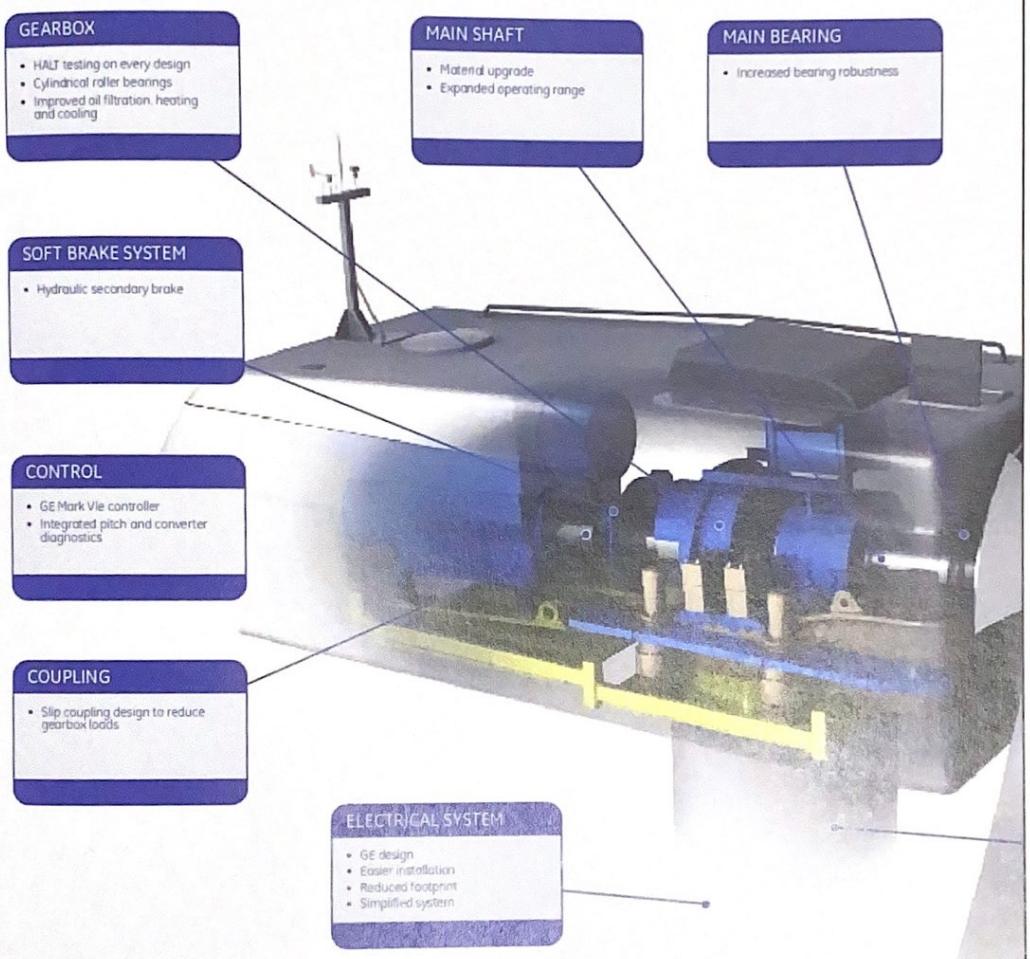

6

Appendix 1.2: Generic 1.5 MW Wind Turbine Technical Datasheet